

This is a PDF file of the unedited manuscript that was accepted for publication:

Feasibility of using rural waste products to increase the denitrification efficiency in a surface flow constructed wetland.

Rosanna Margalef-Marti, Raúl Carrey, Daniel Merchán, Albert Soler, Jesús Causapé, Neus Otero

Journal of Hydrology, 2019, Volume 578, 124035
DOI: <https://doi.org/10.1016/j.jhydrol.2019.124035>

Received date: 23 April 2019

Revised date: 7 August 2019

Accepted date: 9 August 2019

Available online: 13 August 2019

© 2019. This manuscript version is made available under the CC-BY-NC-ND 4.0 license <http://creativecommons.org/licenses/by-nc-nd/4.0/>

1 **Feasibility of using rural waste products to increase the denitrification efficiency in a**
2 **surface flow constructed wetland**

3 Rosanna Margalef-Martí¹, Raúl Carrey¹, Daniel Merchán², Albert Soler¹, Jesús Causapé³, Neus
4 Otero^{1,4}

5 ¹ Grup MAiMA, SGR Mineralogia Aplicada, Geoquímica i Geomicrobiologia, Departament de
6 Mineralogia, Petrologia i Geologia Aplicada, SIMGEO UB-CSIC, Facultat de Ciències de la Terra,
7 Universitat de Barcelona (UB), C/Martí i Franquès s/n, 08028, Barcelona, Spain

8 ² Department of Engineering, IS-FOOD Institute (Innovation & Sustainable Development in Food
9 Chain), Public University of Navarre, Campus de Arrosadia, 31006, Pamplona, Navarra, Spain

10 ³ Geological Survey of Spain—IGME, C/Manuel Lasala 44 9^aB, 50006, Zaragoza, Spain

11 ⁴ Serra Húnter Fellowship, Generalitat de Catalunya, Spain.

12 **ABSTRACT**

13 A surface flow constructed wetland (CW) was set in the Lerma gully to decrease nitrate (NO₃⁻)
14 pollution from agricultural runoff water. The water flow rate and NO₃⁻ concentration were
15 monitored at the inlet and the outlet, and sampling campaigns were performed which consisted
16 of collecting six water samples along the CW flow line. After two years of operation, the NO₃⁻
17 attenuation was limited at a flow rate of ~2.5 L/s and became negligible at ~5.5 L/s. The present
18 work aimed to assess the feasibility of using rural waste products (wheat hay, corn stubble, and
19 animal compost) to induce denitrification in the CW, to assess the effect of temperature on this
20 process, and to trace the efficiency of the treatment by using isotopic tools. In the first stage,
21 microcosm experiments were performed. Afterwards, the selected waste material was applied in
22 the CW, and the treatment efficiency was evaluated by means of a chemical and isotopic
23 characterization and using the isotopic fractionation (ε) values calculated from laboratory
24 experiments to avoid field-scale interference. The microcosms results showed that the stubble
25 was the most appropriate material for application in the CW, but the denitrification rate was found
26 to decrease with temperature. In the CW, biostimulation in autumn-winter promoted NO₃⁻
27 attenuation between two weeks and one month (a reduction in NO₃⁻ between 1.2 and 1.5 mM

28 was achieved). After the biostimulation in spring-summer, the attenuation was maintained for
29 approximately three months (NO_3^- reduction between 0.1 and 1.5 mM). The $\epsilon^{15}\text{N}_{\text{NO}_3/\text{N}_2}$ and
30 $\epsilon^{18}\text{O}_{\text{NO}_3/\text{N}_2}$ values obtained from the laboratory experiments allowed to estimate the induced
31 denitrification percentage. At an approximate average flow rate of 16 L/s, at least 60 % of NO_3^-
32 attenuation was achieved in the CW. The field samples exhibited a slope of 1.0 for $\delta^{18}\text{O}-\text{NO}_3^-$
33 versus $\delta^{15}\text{N}-\text{NO}_3^-$, similar to those of the laboratory experiments (0.9-1.2). Plant uptake seemed
34 to play a minor role in NO_3^- attenuation in the CW. Hence, the application of stubble in the CW
35 allowed the removal of large amounts of NO_3^- from the Lerma gully, especially when applied
36 during the warm months, but its efficacy was limited to a short time period (up to three months).

37 **Keywords:** denitrification, constructed wetland, electron donor, isotopic fractionation,
38 remediation.

39 1. INTRODUCTION

40 Since nitrate (NO_3^-) is known to cause ecological and human health problems (Vitousek et al.,
41 1997; Ward et al., 2005), the presence of this nutrient in water bodies worldwide is a matter of
42 concern. The extensive application of synthetic and organic fertilizers is a major source of NO_3^-
43 pollution. Therefore, agricultural runoff water should be treated before it is drained into larger
44 water bodies such as aquifers, rivers, and/or lakes. Constructed wetlands (CWs) are considered
45 promising, low cost systems for the remediation of diverse water pollutants, are simple to operate,
46 and have low energy requirements (Wu et al., 2015). Hence, directing agricultural runoff water
47 through a CW could be useful for removing NO_3^- to minimize pollution.

48 The surface flow CWs consists of free surface water flowing horizontally through an artificial pond
49 containing floating and/or emergent rooted vegetation and a high diversity of microorganisms
50 (Ilyas and Masih, 2017; Sirivedhin and Gray, 2006; Vymazal, 2007). The main processes that
51 might contribute to NO_3^- pollution mitigation in surface flow CWs are plant uptake, assimilation by
52 microorganisms, and denitrification (Rogers et al., 1991). The latter refers to the reduction of NO_3^-
53 by microorganisms through a series of enzymatic reactions involving the intermediates NO_2^- , NO ,
54 and N_2O , before finally being reduced to N_2 (Knowles, 1982). Parameters such as temperature,
55 dissolved oxygen (O_2), NO_3^- loading, the source and amount of organic carbon (C), microbial
56 species, the type and density of macrophytes, wetland age, and hydraulic conditions play key

57 roles in the NO_3^- removal efficiency (Bachand and Horne, 1999; Beutel et al., 2009; Kong et al.,
58 2009; Sirivedhin and Gray, 2006). Different approaches can be implemented to enhance water
59 remediation, but strategies directed toward the induction of bacterial NO_3^- respiration are
60 preferred since denitrification is an authentic N sink in water, unlike biomass sequestration (Scott
61 et al., 2008). N storage by plants is generally considered temporary, because organic N returns
62 to the system after the death and decay of plants if they are not harvested (Cooper and Cooke,
63 1984; Gumbricht, 1993).

64 In CWs, macrophytes are able not only to assimilate NO_3^- , but also to promote denitrification
65 efficiency. Plants exert an influence on the diversity of microbial species and their enzymatic
66 activities by releasing exudates and oxygen to the rhizosphere (Kong et al., 2009, and references
67 therein), and decomposed plant material can be used by microbes as a source of organic C. For
68 this reason, increased NO_3^- removal is usually found in vegetated CWs relative to that in non-
69 vegetated systems (Jacobs and Harrison, 2014; Soana et al., 2017). If the CW cannot provide
70 enough organic C to support complete denitrification (e.g., from inlet water, soil, plant root
71 exudates, and decomposed vegetal material), the addition of an external organic C source as an
72 electron donor could enhance the heterotrophic denitrification efficiency (Lu et al., 2009; Si et al.,
73 2018). Since the use of pure reagents such as glucose, acetate, or ethanol may be expensive in
74 long-term treatments, the use of industrial or agricultural residues that are rich in organic C could
75 represent a more sustainable solution. Solid products such as animal or vegetal waste (Grau-
76 Martínez et al., 2017; Si et al., 2018; Trois et al., 2010), as well as industrial liquid by-products
77 (Carrey et al., 2018; Margalef-Marti et al., 2019), have already been reported as being useful for
78 promoting denitrification.

79 The pollutant removal efficiency in CWs can be estimated by monitoring the inlet and outlet
80 concentrations of the pollutant (Kovacic et al., 2000; Tanner et al., 2005; Uusheimo et al., 2018).
81 However, this method does not reveal the specific processes involved in the attenuation, making
82 it challenging to focus on the improvement of the wetland design and operation. Stable isotope
83 analyses can provide information on the NO_3^- transformation pathways. In the course of
84 denitrification, the unreacted residual NO_3^- becomes enriched in the heavy isotopes ^{15}N and ^{18}O ,
85 permitting the distinction between biological attenuation and other processes such as dilution
86 which could also lead to decreases in concentration without influencing the isotopic signature

87 (Böttcher et al., 1990; Fukada et al., 2003; Mariotti et al., 1981; Aravena and Robertson, 1998).
88 In plants, significant enrichment in both ^{15}N and ^{18}O is observed in the NO_3^- extracted from leaves
89 after uptake relative to the NO_3^- from water, but the changes in the NO_3^- isotopic composition in
90 the water are minor (Estrada et al., 2017; Spoelstra et al., 2010). Therefore, the NO_3^- isotopic
91 characterization of water samples collected at the CW might improve the understanding and
92 support the evaluation of the performance of the remediation strategy.

93 In this context, the present work was developed to assess the feasibility of using rural waste
94 products (wheat hay, corn stubble, and animal compost) to induce denitrification in a surface flow
95 CW, and to trace the treatment efficiency in the autumn-winter and spring-summer seasons. In
96 the first stage, lab-scale experiments were performed to identify the most appropriate electron
97 donor to be applied in the CW, and to evaluate the effect of temperature on NO_3^- reduction. The
98 isotopic fractionations (ϵ) of N and O of dissolved NO_3^- under each condition were also
99 determined. In the second stage, the selected material was applied in the CW and the treatment
100 efficiency was evaluated by means of a chemical and isotopic characterization using the ϵ values
101 calculated from the laboratory experiments.

102 **2. METHODS**

103 *2.1. Laboratory experiments*

104 Six types of batch experiments were performed in 150 mL crystal Pyrex® bottles crimp-sealed
105 with butyl rubber stoppers under an argon (Ar) headspace. Each microcosm contained 100 mL
106 of water (2 mM NO_3^-) collected from the inlet of the studied CW (see Section 2.2) and a specific
107 C source: corn stubble (1 g); wheat hay (1 g); or animal compost (0.25 g). The six series of parallel
108 experiments were determined according to the waste product employed and the incubation
109 temperature. Series I (C-24) and II (H-24) contained animal compost and wheat hay, respectively,
110 and were incubated at 24 °C; series III (S-24), IV (S-16), and V (S-8) contained corn stubble and
111 were incubated at 24 °C, 16 °C, and 8 °C, respectively; series VI (DS-24) contained partially
112 decomposed corn stubble and was incubated at 24 °C. The partially decomposed stubble was
113 obtained from the CW 7.5 months after its application on September 25, 2017 (see Section 2.2).
114 All series included at least eight replicates of the biostimulated microcosms. Control microcosms
115 for each tested material were prepared using deionized water (DIW) to discard the potential

116 supply of N from the waste products. The detailed content of each microcosm is described in
117 **Table 1**. During incubation, all microcosms were maintained in darkness and under constant
118 vibratory shaking. The biostimulated microcosms were sacrificed at time intervals depending on
119 the denitrification dynamics until complete NO_3^- and NO_2^- removals were achieved. The control
120 microcosms were sacrificed at the end of the biostimulation experiments. Water samples from
121 batch experiments were analyzed for major anions (NO_3^- , NO_2^- , Cl^- , and SO_4^{2-}), ammonium
122 (NH_4^+), non-purgeable dissolved organic C (NPDOC), dissolved inorganic C (DIC), major cations,
123 trace elements, $\delta^{15}\text{N}\text{-NO}_3^-$, $\delta^{18}\text{O}\text{-NO}_3^-$, and $\delta^{13}\text{C}\text{-DIC}$. Samples from control microcosms were
124 analyzed for major anions and NPDOC. The gas accumulated in the headspace of the vials was
125 collected and analyzed for nitrous oxide (N_2O) concentration. The three organic C sources were
126 analyzed for C and N concentrations and $\delta^{13}\text{C}\text{-C}_{\text{bulk}}$ and $\delta^{15}\text{N}\text{-N}_{\text{bulk}}$.

127 2.2. CW test

128 In the 2000s, approximately 20,000 ha of rainfed croplands were transformed into irrigated
129 agricultural land in the Arba River Basin (Zaragoza, Spain). A small watershed representative of
130 the area (Lerma basin, 733 ha) was monitored to assess the effects of this transformation on the
131 water balance and the salt and NO_3^- -N exports (Merchán et al., 2015, 2014, 2013). In general,
132 the implementation of irrigation implied a three-fold increase in N export to the receiving water
133 bodies, in this case the Arba River, which was the first surface water body in the Ebro River Basin
134 to be declared affected by NO_3^- pollution according to the Nitrates Directive 91/676/EEC. In order
135 to diminish the release of NO_3^- from the Lerma Basin to the Arba River, a surface flow CW was
136 constructed in October 2015, initially covering an area of $\sim 1500\text{ m}^2$, and was enlarged in June
137 2017, covering a final area of $\sim 2500\text{ m}^2$ with a depth of $\sim 40\text{ cm}$. The surface water of the Lerma
138 gully can be partially diverted towards the CW. Water flow in the Lerma gully varies between 15
139 and 60 L/s. Temperature and precipitation data collected monthly in the area are reported in
140 Supporting information (**Table S1**).

141 The CW is fully automated, with high-frequency monitoring (every 10 minutes) of the water flow
142 rate and NO_3^- concentration at both the inlet and the outlet. Emergent macrophytes (*Typha* and
143 *Phragmites*) started growing since its construction, and occupied approximately 75 % of the CW
144 surface at the time the present study began, since the enlarged part was still unvegetated. The

145 field survey was performed in three periods and involved 13 sampling campaigns, each consisting
146 of the collection of six water samples (H1 to H6) from along the wetland flow line (**Figure 1**). In
147 the first period (June to September 2017), two different operating conditions were tested before
148 the biostimulation by modifying the inlet opening; three sampling campaigns were performed at
149 two different flow rates (~5.5 L/s and ~2.5 L/s). The second period involved the application of corn
150 stubble obtained from the surrounding crops (~8000 kg) on September 25, 2017, and the
151 evaluation of treatment efficiency by performing two sampling campaigns 7 and 14 d after the
152 application. The third period involved a second application of corn stubble (~6000 kg) on May 11,
153 2018, and the evaluation of treatment efficiency by performing eight sampling campaigns from
154 May 2018 to October 2018. In the two biostimulation periods, the corn stubble was applied over
155 all the CW surface between H1 and H3. Throughout these second and third periods, the CW was
156 operated at a higher flow rate (~16 L/s). The given flow rate for the CW test periods is that
157 measured at the outlet. The calculated residence time of NO_3^- in the CW was 21, 51 and 112 h
158 for the tested flow rates of 16, 5.5 and 2.5 L/s, respectively. Detailed information about the
159 sampling campaigns is shown in **Table 2**. Water samples collected at the CW were analyzed for
160 major anions (NO_3^- , NO_2^- , Cl^- , and SO_4^{2-}), NH_4^+ , NPDOC, DIC, major cations, trace elements,
161 $\delta^{15}\text{N-NO}_3^-$, $\delta^{18}\text{O-NO}_3^-$, $\delta^{34}\text{S-SO}_4^{2-}$, $\delta^{18}\text{O-SO}_4^{2-}$, and $\delta^{13}\text{C-DIC}$.

162 2.3. Analytical methods

163 Water samples for the field and laboratory batch experiments were immediately filtered through
164 0.2 μm Millipore® filters after being collected, and were stored at 4 °C until analysis. The aliquots
165 for NH_4^+ , $\delta^{15}\text{N-NO}_3^-$, and $\delta^{18}\text{O-NO}_3^-$ analysis were frozen, and the aliquots for the DIC and $\delta^{13}\text{C-}$
166 DIC analyses were left with no headspace and stored at 4 °C.

167 Anions (Cl^- , NO_2^- , NO_3^- , and SO_4^{2-}) were analyzed by high-performance liquid chromatography
168 (HPLC) (Waters 515 pump and Waters IC-Pak anion column with Waters 432 and KONTRON
169 UV/Vis detectors). NH_4^+ was analyzed by three techniques due to equipment availability issues:
170 I) spectrophotometry using the indophenol blue method (CARY 1E UV-visible), II) ion
171 chromatography or III) ammonia ion selective electrode (ORION, Thermo Scientific). DIC was
172 analyzed by titration (METROHM 702 SM Titrino), NPDOC by organic matter combustion (TOC
173 500 SHIMADZU), and major cations and trace elements by ICP-OES (Perkin Elmer Optima 8300).

174 The concentration of N₂O accumulated at the headspace of the vials was analyzed by gas
175 chromatography (GC) (Thermo Scientific Trace 1300 with ECD detector), and C and N
176 concentrations in the waste materials employed as C sources were analyzed with an elemental
177 analyzer (EA) (Carlo Erba1108 CHNS-O EA). The $\delta^{15}\text{N-NO}_3^-$ and $\delta^{18}\text{O-NO}_3^-$ were determined
178 following the cadmium and azide reduction method (McIlvin and Altabet, 2005; Ryabenko et al.,
179 2009). The isotopic composition of the N₂O obtained from the NO₃⁻ reduction was analyzed using
180 a Pre-Con coupled to a Finnigan MAT 253 isotope ratio mass spectrometer (IRMS) (Thermo
181 Scientific). For the SO₄²⁻ isotopic analysis, the dissolved SO₄²⁻ was precipitated as BaSO₄ by
182 adding BaCl₂·2H₂O after acidifying the sample with HCl and boiling it in order to prevent
183 precipitation of BaCO₃ (Dogramaci et al., 2001). The $\delta^{34}\text{S-SO}_4^{2-}$ was analyzed with a Carlo Erba
184 EA coupled in continuous flow to a Finnigan Delta XP Plus IRMS, whereas the $\delta^{18}\text{O-SO}_4^{2-}$ was
185 analyzed with a ThermoQuest high-temperature conversion analyzer (TC/EA) coupled in
186 continuous flow to a Finnigan Matt Delta XP Plus IRMS. The $\delta^{13}\text{C-DIC}$ was analyzed via
187 carbonate conversion to CO₂ gas by adding a phosphoric acid solution and measuring the gas
188 evolved with a Gas-Bench II coupled to a MAT-253 IRMS (Thermo Scientific). The $\delta^{13}\text{C-C}_{\text{bulk}}$ and
189 $\delta^{15}\text{N-N}_{\text{bulk}}$ of the waste materials employed as C sources were determined with a Carlo Erba EA
190 coupled to a Finnigan Delta C IRMS.

191 The isotopic notation is expressed in terms of δ (‰) relative to the international standards:
192 atmospheric N₂ (AIR) for $\delta^{15}\text{N}$, Vienna Standard Mean Oceanic Water (V-SMOW) for $\delta^{18}\text{O}$,
193 Vienna Pee Dee Belemnite (V-PDB) for $\delta^{13}\text{C}$, and Vienna Canyon Diablo Troillite (V-CDT) for
194 $\delta^{34}\text{S}$. Hence, $\delta = ((R_{\text{sample}}-R_{\text{standard}})/R_{\text{standard}})$, where R is the ratio between the heavy and the light
195 isotopes. Following Coplen (2011), several international and laboratory (CCiT) standards were
196 interspersed among the samples for normalization of the results (Supporting Information **Table**
197 **S2**). The reproducibilities (1 σ) of the samples, calculated from the standards systematically
198 interspersed in the analytical batches, were ± 1.0 ‰ for $\delta^{15}\text{N-NO}_3^-$, ± 1.5 ‰ for $\delta^{18}\text{O-NO}_3^-$, ± 0.2 ‰
199 for $\delta^{15}\text{N-N}_{\text{bulk}}$, ± 0.2 ‰ for $\delta^{13}\text{C-C}_{\text{bulk}}$, ± 0.2 ‰ for $\delta^{13}\text{C-DIC}$, ± 0.2 ‰ for $\delta^{34}\text{S-SO}_4^{2-}$, and ± 0.5 ‰ for
200 $\delta^{18}\text{O-SO}_4^{2-}$. Samples for chemical and isotopic analyses were prepared at the laboratory of the
201 MAiMA-UB research group, and analyzed at the Centres Científics i Tecnològics of the Universitat
202 de Barcelona (CCiT-UB).

203 3. RESULTS AND DISCUSSION

204 3.1. Lab-scale evaluation of the nitrate removal capacities of compost, hay, and stubble at 24 °C

205 The chemical and isotopic characterization of the samples obtained from the laboratory
206 experiments are presented in the Supporting Information (**Table S3**). Although the intrinsic N
207 content measured in the three waste products (stubble, hay, and compost) were low (**Table 3**), it
208 was not possible to disregard a certain supply of N from these materials throughout the
209 incubations. The control microcosms containing the three C sources and DIW showed NO_3^- , NO_2^-
210 , and NH_4^+ concentrations below 0.09 mM, 0.02 mM, and 0.12 mM, respectively.

211 The biostimulation experiments showed that the three tested C sources were able to promote
212 NO_3^- removal. Complete denitrification (total NO_3^- and NO_2^- removal) was reached in
213 approximately 40 h in the microcosms containing stubble and hay, and in approximately 95 h in
214 that containing compost (**Figure 2A**). NH_4^+ was detected in some of the samples (in
215 concentrations of up to 1 mM), but with no clear pattern, suggesting the possible coexistence of
216 denitrification and dissimilatory NO_3^- reduction to NH_4^+ (DNRA) and/or the input of NH_4^+ -N
217 supplied from the C sources tested. Transient NO_2^- accumulation of up to 1.5 mM (stubble and
218 hay) and 0.7 mM (compost) were observed. The highest concentration of NO_2^- in the stubble and
219 hay microcosms were detected after complete NO_3^- reduction, and subsequently decreased to
220 below the detectable limit in less than 40 h from the beginning of the experiment. Contrarily, in
221 the microcosms containing compost, the highest NO_2^- concentration was observed after 40 h,
222 and thereafter decreased along with NO_3^- concentration until both compounds were below the
223 detectable limits, after 96 h. The differences in NO_2^- accumulation between the compost, stubble,
224 and hay experiments were likely related to the rate of NO_3^- reduction. NO_2^- accumulation has
225 been reported to depend on the relative rates of NO_3^- and NO_2^- reduction (Betlach and Tiedje,
226 1981), as well as on the type of C source and C/N ratios employed (Akunna et al., 1993; Ge et
227 al., 2012). The slower reduction observed with compost could be due to the lower amount of
228 material used in the experiments (0.25 g instead of the 1 g used for stubble and hay). Although
229 the intrinsic C concentrations of the three sources were similar (**Table 3**), the C bioavailability
230 could differ between each product, and even between replicates, due to heterogeneity in the
231 materials (Breulmann et al., 2014; Sobczak and Findlay, 2002; Warneke et al., 2011).
232 Consequently, the NPDOC concentration did not show a clear correlation with NO_3^- reduction,
233 but provided an approximation of the amount of added C present in dissolved form. Although the

234 quantity of compost in the microcosms was only one-quarter of the quantity of vegetal materials
235 used, the measured NPDOC concentrations in the three types of microcosms were similar (13.2-
236 27.3 mM for stubble, 11.8-16.8 mM for hay, and 5.3-14.3 mM for compost). The $\delta^{13}\text{C}$ -DIC
237 provided information about the transformation of organic C from the waste materials to inorganic
238 C; a brief discussion is presented in the Supporting Information (**section S1**).

239 Concerning the safety of the materials, the ICP-OES analyses showed that there was no release
240 of toxic trace elements from any of the tested compounds (Supporting Information **Table S4**). Hay
241 and stubble seemed to be more feasible than compost for application in the CW. Compost
242 resulted in a lower denitrification rate, the NO_2^- accumulation lasted longer, and it was highly
243 soluble and could be rapidly removed from the CW via the water flow. In this study, stubble was
244 selected for application in the studied CW due to a higher availability in the area. Therefore, further
245 experiments were only performed with stubble.

246 *3.2. Lab-scale evaluation of the effect of temperature on denitrification induction by stubble*

247 The denitrification activity of microorganisms is usually increased with higher temperatures, and
248 therefore higher NO_3^- attenuation from water can be observed during warm periods (Rivett et al.,
249 2008; Spieles and Mitsch, 1999). To assess the effect of temperature on the induced
250 denitrification strategy, additional experiments were performed. A comparison between different
251 incubation temperatures in corn stubble experiments showed that denitrification reached
252 completion across the whole temperature range studied (from 8 to 24 °C), but with different lag
253 periods and NO_3^- reduction rates. Complete denitrification was achieved after 40 h at 24 °C, 65 h
254 at 16 °C, and 140 h at 8 °C (**Figure 2B**). The decrease in NO_3^- began after 10 h at 24 °C, whereas
255 at 16 °C and 8 °C lag periods of 45 h and 79 h, respectively, were observed. A decrease in NO_3^-
256 reduction rate associated with lower temperatures following the Arrhenius relationship has been
257 well documented (Dawson and Murphy, 1972). Therefore, the denitrification efficiency might
258 decrease during the winter months or low-temperature periods in comparison to that during the
259 summer months, and thus application of the carbon source throughout the spring months might
260 be advantageous. Significant transient NO_2^- accumulation (up to 1.5 mM at 24 °C, 1.8 mM at 16
261 °C, and 1.0 mM at 8 °C) was observed in all the experiments. As discussed in the previous section,
262 NO_2^- accumulation was less significant in the experiment with a lower denitrification rate (8 °C).

263 3.3. *Lab-scale assessment of the lifespan of the denitrification induced by stubble*

264 One of the main issues associated with biostimulation strategies is their effectiveness during long-
265 term treatments. It is thus important to consider the lifespan of the material to be employed in the
266 CW. In another laboratory experiment with vegetable materials (palm leaves and compost),
267 induced NO_3^- degradation was shown to be maintained for more than 220 d (Grau-Martínez et
268 al., 2017). In this context, microcosms containing partially decomposed stubble (sampled in the
269 CW 7.5 months after its application) were incubated and compared to microcosms containing
270 fresh stubble. The denitrification induced by the partially decomposed stubble proceeded at a
271 higher rate than that induced by the fresh stubble; complete NO_3^- reduction was achieved in less
272 than 25 h with the former, instead of 40 h with the latter (**Figure 2B**). In the partially decomposed
273 stubble microcosms, transient NO_2^- accumulation was below 0.8 mM. Due to the increased
274 heterogeneity of the material after being in the field and in contact with water for months, high
275 variabilities in both NO_3^- and NO_2^- concentrations were observed between replicates. Therefore,
276 the reduction rates obtained from these experiments must be considered approximations. These
277 results showed that the intrinsic capacity of the stubble to promote denitrification after 7.5 months
278 being in contact with water was still important, at least at lab-scale. However, the NPDOC content
279 in the microcosms containing partially decomposed stubble (1.7-8.8 mM) were lower than those
280 in the microcosms with fresh stubble incubated at 24 °C (13.2-27.3 mM), pointing to a decreased
281 availability of the electron donor over time. In the CW, the specific lifespan of the treatment might
282 be shorter, since the organic C also typically consumes O_2 before using NO_3^- as an electron
283 donor. The N_2O accumulated in the headspace of the microcosms containing partially
284 decomposed stubble incubated at 24 °C (as well as that in the microcosms containing fresh
285 stubble incubated at 16 and 8 °C) was also measured since the release of greenhouse gases
286 during N transformation processes is a matter of concern. The maximum N_2O concentration
287 detected accounted for 0.015 % of the initial N- NO_3^- content of the microcosms (Supporting
288 Information (**Table S3**)).

289 3.4. *Lab-scale: NO_3^- isotopic fractionation calculation.*

290 Under closed-system conditions, the isotopic fractionation (ϵ) for a determined element (e.g., N
291 and O from dissolved NO_3^-) can be calculated by means of a Rayleigh distillation equation

292 **(Equation 1)**. Thus, ϵ can be obtained from the slope of the linear correlation between the natural
 293 logarithm of the remaining substrate fraction ($\text{Ln}(C_{\text{residual}}/C_{\text{initial}})$, where C refers to analyte
 294 concentration) and the determined isotope ratios ($\text{Ln}(R_{\text{residual}}/R_{\text{initial}})$, where $R = \delta + 1$). These
 295 $\epsilon^{15}\text{N}_{\text{NO}_3/\text{N}_2}$ and $\epsilon^{18}\text{O}_{\text{NO}_3/\text{N}_2}$ values, determined at lab-scale under controlled conditions, can be later
 296 applied at field-scale to estimate the contribution of denitrification to the NO_3^- attenuation, while
 297 avoiding field-scale interference such as dilution due to rainfall (Böttcher et al., 1990; Mariotti et
 298 al., 1988). We calculated $\epsilon^{15}\text{N}_{\text{NO}_3/\text{N}_2}$ and $\epsilon^{18}\text{O}_{\text{NO}_3/\text{N}_2}$ under all tested conditions at lab-scale (**Figure**
 299 **3**) to appropriately evaluate the efficacy of the induced denitrification strategy tested at the CW.
 300 A summary of the calculated $\epsilon^{15}\text{N}_{\text{NO}_3/\text{N}_2}$, $\epsilon^{18}\text{O}_{\text{NO}_3/\text{N}_2}$, and $\epsilon^{15}\text{N}/\epsilon^{18}\text{O}$ values is shown in (**Table 4**);
 301 $\epsilon^{15}\text{N}_{\text{NO}_3/\text{N}_2}$ ranged from -31.9 to -10.5‰, $\epsilon^{18}\text{O}_{\text{NO}_3/\text{N}_2}$ from -30.4 to -9.7‰, and $\epsilon^{15}\text{N}/\epsilon^{18}\text{O}$ from 0.8 to
 302 1.8. These values fall within the reported range for heterotrophic denitrification (see Table 4; Grau-
 303 Martínez et al., (2017)). The lowest $\epsilon^{15}\text{N}_{\text{NO}_3/\text{N}_2}$ and $\epsilon^{18}\text{O}_{\text{NO}_3/\text{N}_2}$ values were found for the
 304 microcosms containing compost incubated at 24 °C and stubble incubated at 8 °C, which were
 305 the two experiments that presented lower NO_3^- reduction rates. Apart from the microcosms
 306 containing stubble incubated at 8 °C, the other microcosms containing stubble (both fresh and
 307 partially decomposed and incubated at 16 or 24 °C) presented narrower ranges of $\epsilon^{15}\text{N}_{\text{NO}_3/\text{N}_2}$ (from
 308 -28.3 to -22.5‰), $\epsilon^{18}\text{O}_{\text{NO}_3/\text{N}_2}$ (from -30.4 to -21.2‰) and $\epsilon^{15}\text{N}/\epsilon^{18}\text{O}$ (from 0.8 to 1.1). These values
 309 were employed to assess the efficiency of the biostimulation strategy at the studied CW.

$$310 \quad \text{Ln} \left(\frac{R_{\text{residual}}}{R_{\text{initial}}} \right) = \epsilon \times \text{Ln} \left(\frac{C_{\text{residual}}}{C_{\text{initial}}} \right) \quad \text{Equation 1}$$

311 *3.5. Performance of the CW before application of stubble*

312 The chemical and isotopic characterization of the samples obtained from the CW both before and
 313 after application of the electron donor are presented in Supporting Information (**Table S5**). Three
 314 sampling campaigns were performed at the CW before stubble application. While NO_3^- was not
 315 significantly reduced during the two sampling campaigns performed at a ~5.5 L/s flow rate (June
 316 and September 2017), a slight attenuation (from 1.3 to 0.8 mM) occurred under operation at ~2.5
 317 L/s (September 2017) (**Figure 4A**). In all samples, NO_2^- was below the detection limit and NH_4^+
 318 was below 0.01 mM, suggesting that NO_3^- had been either transformed to gaseous N products
 319 through denitrification or assimilated by plants or microorganisms (Supporting information (**Table**
 320 **S5**)). Whereas no increase in $\delta^{15}\text{N}-\text{NO}_3^-$ nor $\delta^{18}\text{O}-\text{NO}_3^-$ was observed in the samples collected

321 during the first campaign at ~5.5 L/s (June 14, 2017), an increase was observed at the middle
322 section of the CW (H3) during the second survey at ~5.5 L/s (September 5, 2017). In this latter
323 campaign, the inlet (H1) presented $\delta^{15}\text{N-NO}_3^-$ and $\delta^{18}\text{O-NO}_3^-$ values of +11.6 ‰ and +8.7 ‰,
324 respectively, which increased at the middle point (H3) up to +19.2 ‰ and +18.2 ‰, respectively,
325 and decreased at the outlet (H6) to +9.6 ‰ and +7.1 ‰, respectively (**Figure 4B**). A proposed
326 explanation is that the occurrence of preferential flows within the wetland (e.g., heterogeneous
327 flow rate between surface and bottom water or between lateral and central water) could have led
328 to an increased hydraulic retention time and/or stagnant water at the H3 sampling site. In the
329 campaign performed at a ~2.5 L/s flow rate (September 12, 2017), the decrease in NO_3^-
330 concentration was coupled to increases in $\delta^{15}\text{N-NO}_3^-$ and $\delta^{18}\text{O-NO}_3^-$ from the inlet (+7.0 ‰ and
331 +4.7 ‰, respectively, at H1) to the outlet (+17.1 ‰ and +13.0 ‰, respectively, at H6) of the CW
332 (**Figure 4B**). The slope of the relation between $\delta^{18}\text{O-NO}_3^-$ and $\delta^{15}\text{N-NO}_3^-$ for the samples
333 collected in these three campaigns was 0.8 ($r^2 = 0.91$) (**Figure 4B**), which is indicative of
334 denitrification activity (Aravena et al., 1998). These results are in agreement with previous results
335 reporting the occurrence of denitrification in CWs even in the presence of dissolved O_2 (Sirivedhin
336 and Gray, 2006). The intrinsic denitrification activity in the CW did not support complete
337 denitrification, likely due to the low NPDOC content of the water (0.4 – 0.6 mM). Therefore, it was
338 decided to evaluate the feasibility of adding an external electron donor source to promote NO_3^-
339 attenuation when operating at a ~16 L/s flow rate.

340 3.6. Performance of the CW after application of stubble

341 Application of stubble in autumn (September 25, 2017) induced denitrification in the CW
342 approximately 2 d after the application (**Figure 5B**). Denitrification was almost complete at the
343 outlet (H6) by 14 d following the application (0.2 mM NO_3^- remaining of the initial 1.4 – 1.7 mM)
344 (**Figure 5A**). In the two sampling campaigns, NO_2^- accumulated beginning at H2 and reached a
345 concentration of 0.2 mM by the outlet (H6) by 7 d after treatment, but decreased to 0.1 mM by 14
346 d. Such a decrease in NO_2^- accumulation over time has been previously observed in laboratory
347 experiments and other denitrification studies (Carrey et al., 2014; Margalef-Marti et al., 2019;
348 Vidal-Gavilan et al., 2013). The maximum NH_4^+ concentration of 0.02 mM was measured at H3
349 after 7 d, while it decreased by the outlet (H6) to 0.01 mM in both campaigns, pointing to a non-
350 significant contribution of DNRA. Due to the application of stubble, the outlet flow rate decreased

351 until the system became partially blocked, leaving the monitoring probes exposed to the air. When
352 the problem was solved (October 17, 2017) and the outlet flow was stabilized at approximately
353 16 L/s, the NO_3^- concentration monitored at the outlet showed fluctuations, pointing to a slight
354 denitrification activity until October 24, 2017 (**Figure 5C**). Thus, the lifetime of the treatment in
355 autumn (recorded temperatures in October 2017 ranged from 10.3 °C to 20.4 °C, averaging 16.0
356 °C) was estimated to be between 2 weeks and 1 month.

357 Application of stubble in spring (May 5, 2018) also induced denitrification and underwent a shorter
358 acclimation time (1 d) with respect to the first application, likely due to faster acclimation by the
359 previously stimulated bacterial community (**Figure 6A**). By 7 d after the stubble application, the
360 NO_3^- concentration at the outlet (H6) was 0.2 mM, and denitrification was complete after 14 d.
361 The NO_3^- concentration in the outlet then began to increase progressively until reaching a level
362 similar to that at the inlet by approximately 100 d after treatment (**Figure 6B**). A lower NO_3^-
363 concentration measured in H3 during the last sampling campaign (+161 d) was attributed to
364 stagnant water near the sampling point due to the accumulation of partially decomposed stubble.
365 Thus, the treatment in spring-summer (temperatures recorded from May to October 2018
366 presented monthly minimums from 9.6 to 19.9 °C, monthly maximums from 20.0 to 28.4 °C, and
367 monthly averages from 15.8 to 24.6 °C) induced significant denitrification for approximately three
368 months, which is three times longer than that induced by the treatment in autumn. The NO_3^-
369 concentration decrease at the outlet compared to inlet during these three months ranged from 0.1
370 to 1.5 mM (highest attenuation corresponded to the first month after stubble application). All the
371 monitored NO_3^- concentrations at the inlet and outlet of the CW during this study period are
372 presented in the Supporting Information **Figure S1**. The increased efficiency of the treatment in
373 spring-summer compared to that of the treatment in autumn is in accordance with laboratory
374 results (incubation at 8, 16, and 24 °C) and with previous wetland studies reporting increased
375 denitrification rates at higher temperatures (Bachand and Horne, 1999; Christensen and Srensen,
376 1986; Si et al., 2018). The faster acclimation by the previously stimulated bacterial community
377 could have been also responsible for this increased attenuation activity.

378 After the second stubble application, 0.1 mM of NO_2^- was detected at the outlet (H6) for 63 d.
379 Afterwards, it was no longer detected (except at the aforementioned point H3 where water
380 stagnated), confirming a decreased NO_2^- accumulation with time as observed during the previous

381 treatment period. The maximum NH_4^+ concentration detected, 0.3 mM, was recorded at H4 7 d
382 after application, while at the outlet (H6), the concentration was 0.05 mM. At 14 d and one month
383 after application, NH_4^+ at the outlet decreased to 0.02 mM and 0.01 mM, respectively. These
384 results suggest that transient DNRA activity could have arisen between H2 and H4 following the
385 stubble application. NO_3^- is reduced to NH_4^+ through DNRA, depending on parameters such as
386 microbial growth rate, NO_2^- accumulation, and the C:N ratio (Kraft et al., 2014). It is generally
387 accepted that DNRA is favored at high C:N ratios, when NO_3^- is limited (rather than the electron
388 donor being limited), or when high NO_3^- levels inhibit NO_2^- reductase (Giles et al., 2012; Kelso et
389 al., 1997). This hypothesis is consistent with the higher degree of NH_4^+ accumulation observed
390 in laboratory experiments compared to that observed in the field, since higher C:N ratios with a
391 more homogeneous distribution were found in the batch experiments. It is also necessary to
392 account for the possible input of N from the applied stubble. NO_2^- and NH_4^+ have a lower threshold
393 for human consumption (0.01 and 0.03 mM, respectively) with respect to that of NO_3^- (0.8 mM)
394 (98/83/EC, 1998). However, since NH_4^+ accumulation decreased before the outlet and fell to
395 insignificant levels by 14 d after treatment, and the NO_2^- accumulation also decreased over time,
396 stubble was considered effective in removing N compounds from agricultural runoff water.

397 A few authors have previously attempted to calculate the denitrification efficiency in CWs by
398 means of isotopic assessment, but using ϵ values available in the literature and only for N- NO_3^-
399 (Lund et al., 1999; Søvik and Mørkved, 2008). The $\epsilon^{15}\text{N}_{\text{NO}_3/\text{N}_2}$ and $\epsilon^{18}\text{O}_{\text{NO}_3/\text{N}_2}$ values obtained from
400 our lab-scale experiments in which fresh stubble was incubated at 24 and 16 °C, and partially
401 decomposed stubble was incubated at 24 °C, were used to calculate three denitrification % lines
402 (**Equation 2**, derived from **Equation 1**) that were plotted on a graph of $\delta^{18}\text{O}-\text{NO}_3^-$ versus $\delta^{15}\text{N}-$
403 NO_3^- along with the isotopic results for the CW samples (**Figure 7**). These three laboratory
404 conditions encompass the average temperatures recorded during the biostimulation periods
405 tested at the CW. The slope of $\delta^{18}\text{O}-\text{NO}_3^-$ versus $\delta^{15}\text{N}-\text{NO}_3^-$ for the field samples collected after
406 the biostimulation treatment was 1.0 ($r^2 = 0.98$) (**Figure 7**), which is slightly higher than that
407 obtained for the intrinsic denitrification before the stubble addition (0.8 ($r^2 = 0.91$)), which is likely
408 due to the use of a different C source and the promotion of a different bacterial community. Also,
409 the slope obtained after the biostimulation (1.0) was similar to the slopes obtained in the lab-scale
410 experiments using partially decomposed stubble incubated at 24 °C (0.9) and those using fresh

411 stubble incubated at 24 and 16 °C (1.25 and 1.1, respectively). This is consistent with the
412 temperatures registered in the area throughout the test period, and with the stubble being in
413 contact with water. This similarity between the field-scale and lab-scale slopes, together with the
414 observed isotopic fractionation in the CW suggested that plant uptake did not likely contribute
415 significantly to the NO₃⁻ removal.

$$416 \text{ Denitrification \%} = \left[1 - \left(\frac{C_{\text{residual}}}{C_{\text{initial}}} \right) \right] \times 100 = \left[1 - e^{\left(\frac{\delta_{\text{residual}} - \delta_{\text{initial}}}{\epsilon} \right)} \right] \times 100$$

417 **Equation 2**

418 The results showed that at least 60% of NO₃⁻ attenuation was achieved in the CW due to the
419 induced denitrification, although this value was obtained from the less-favorable situation (where
420 the denitrification % was calculated from the experiments using stubble incubated at 24 °C). If the
421 denitrification % is instead calculated based on the experiment using partially decomposed
422 stubble incubated at 24 °C, which presents the slope most similar to that of the field samples (0.9
423 compared to 1.0), then denitrification accounted for a 70 % NO₃⁻ removal. The largest contribution
424 of denitrification, as determined by isotopic data, was observed in the outlet samples (H6) taken
425 7 and 14 d after the first stubble application, and 7 d after the second stubble application. By 14
426 d after the second stubble application, NO₃⁻ concentration in some samples was below the level
427 required for the isotopic analysis. Therefore, the induced denitrification allowed a NO₃⁻ attenuation
428 close to 100 %. After two weeks of treatment, the contribution of the induced denitrification at the
429 outlet (H6) began to decrease, from 30 % in June 2018 to 5 % in September 2018, and slightly
430 increased to 20 % by the last survey in October 2018. Considering an average flow rate of 16 L/s
431 (the application of stubble led to fluctuations in the flow rate due to partial blockages at some
432 points caused by stubble accumulation) and these results, in the studied CW, at least 80 kg of
433 NO₃⁻ were removed per day over the first two weeks after the stubble application in May 2018
434 and 30 kg/d were removed from 14 to 63 d after the supply, after which time the removal
435 decreased. A comparison between the denitrification percentages calculated using chemical and
436 isotopic data revealed that using concentration values always resulted in a higher value. Since
437 the contribution calculated from the isotopic data was considered to be linked to NO₃⁻ attenuation
438 due to denitrification, the difference could be due to a decrease in NO₃⁻ concentration provoked
439 by dilution due to precipitation, or the contribution of plant uptake to NO₃⁻ attenuation.

440 3.7. *Effect and evolution of NPDOC in the CW*

441 Since the amount of organic C released from the CW to the Lerma gully, and from there to the
442 Arba River was a matter of concern, the NPDOC concentration in the field samples were
443 measured. Only the results obtained from the second stubble application are discussed (the first
444 application gave similar results). The NPDOC concentration at the outlet increased with respect
445 to the background values by 7 d after application, and the increased level was maintained for 14
446 d in total (**Figure 8**). The increase began at H3, reached a maximum between H4 and H5 (1.6 –
447 1.7 mM), and decreased to approximately 1.0 – 1.1 mM by the outlet (H6), indicating a release of
448 organic C to the gully (background NPDOC concentrations ranged from 0.5 to 0.8 mM). Because
449 the gully contained NO_3^- -polluted water, it was considered that the surplus organic C could lead
450 to NO_3^- attenuation downstream. The high NPDOC concentration detected between H3 and H5
451 could have provoked a decrease in water quality within the CW due to the promotion of processes
452 such as DNRA (previously discussed) and bacterial SO_4^{2-} reduction (BSR), through which NH_4^+
453 and H_2S are produced, respectively. Although BSR is usually induced when NO_3^- is completely
454 removed from the environment, the coexistence of denitrification and BSR in the presence of an
455 abundance of an electron donor has also been demonstrated (Laverman et al., 2012). The
456 isotopic characterization of SO_4^{2-} can provide information to assess its transformation processes
457 because the decrease in SO_4^{2-} concentration is coupled to increases in $\delta^{34}\text{S}\text{-SO}_4^{2-}$ and $\delta^{18}\text{O}\text{-}$
458 SO_4^{2-} through the BSR (Strebel et al., 1990). Correlation between SO_4^{2-} concentration and
459 isotopic composition was not identified in the samples collected at the CW, suggesting that BSR
460 was not occurring in the CW. Therefore, the possibility of a decrease in water quality in the CW
461 due to H_2S production as a result of excess organic C was discarded.

462 3.8. *Suitability of the strategy and future improvements*

463 The remediation strategy tested in the CW allowed the induction of the removal of NO_3^- from
464 agricultural runoff water. The NO_3^- attenuation was primarily related to denitrification. Previous
465 studies also found that denitrification was an important N sink in CWs in comparison to plant
466 uptake (Lin et al., 2002; Soana et al., 2017). It has to be considered that denitrification can only
467 be considered a N sink if intermediate products such as NO_2^- or N_2O are not accumulated during
468 the NO_3^- reduction. The added stubble could have enhanced denitrification not only by increasing

469 the organic C content of the water but also by inhibiting O₂ production through photosynthesis by
470 shading the water column, as previously hypothesized by Jacobs and Harrison (2014) for floating
471 vegetation in CWs. However, the denitrification efficiency was limited. The most likely explanation
472 involves the high O₂ content of the inlet water (near saturation, approximately 0.28 and 0.34 mM
473 in summer and winter, respectively) (Merchán et al., 2014) and the vast surface available for O₂
474 diffusion. Other parameters that could have also contributed to the limited denitrification efficiency
475 include the high water flow rate tested in the CW (~16 L/s), and the possible generation of
476 preferential flows within the CW (e.g., due to stubble accumulation in some points) that could led
477 to a low degree of interaction between water and stubble.

478 Although application of solid residues such as maize stubble in surface flow CWs might have
479 advantages over the application of liquid organic C sources, which face the problems of greater
480 loss by bacterial oxidation (Lin, 2002) and greater release with the water flow, new strategies for
481 increasing the lifespan and efficacy of the induced denitrification must be investigated. In addition,
482 increased intrinsic denitrification capacity of the CW is expected after plant growth covers the
483 entire surface. Previous studies have reported increased denitrification activity in vegetated CWs
484 relative to the levels in non-vegetated systems (Lin et al., 2002; Soana et al., 2017), with efficacy
485 varying among plants of different species or age (Lin et al., 2002; Lund et al., 1999). The organic
486 C pool released after plant senescence has also been demonstrated to increase the bacterial
487 activity, as this C can also be used as electron donor (Peralta et al., 2012; Soana et al., 2017). In
488 this direction, Kang et al. (2018) proposed the use of plants whose growth season is winter.
489 Therefore, the organic C supply from senescence would occur throughout the summer months,
490 when temperatures are higher and more appropriate conditions are established for the promotion
491 of significant denitrification activity.

492 N₂O production was not assessed in our field-scale tests. At lab-scale, limited N₂O production
493 was observed. However, at field-scale, higher N₂O emissions could occur as a result of
494 denitrification induced by the stubble addition because the high O₂ content of the inlet water and
495 the free surface water flow might allow more extensive O₂ diffusion in water. Since N₂O emissions
496 are detrimental for air quality, the production of this greenhouse gas should also be monitored in
497 treatments aiming to induce denitrification. Isotopic characterization of the N₂O emitted from a

498 given CW could also provide further information about the N transformation processes that led to
499 the decrease in NO_3^- concentration.

500 **4. CONCLUSIONS**

501 At laboratory-scale, maize stubble, wheat hay, and animal compost were able to induce complete
502 denitrification. Stubble was selected for field-scale application due to its better local availability.
503 In the following incubations, stubble sampled from the CW 7.5 months after its application was
504 still able to support complete NO_3^- attenuation. Complete NO_3^- attenuation was achieved over
505 the temperature range of 8 to 24 °C, although lower temperatures resulted in lower reduction
506 rates. The $\epsilon^{15}\text{N}_{\text{NO}_3/\text{N}_2}$ and $\epsilon^{18}\text{O}_{\text{NO}_3/\text{N}_2}$ values obtained from the laboratory experiments allowed
507 evaluation of the performance of the remediation strategy at the CW.

508 Before the application of the stubble, NO_3^- attenuation at the CW (from 1.3 to 0.8 mM) was only
509 observed when the flow was decreased from approximately 5.5 to 2.5 L/s. The biostimulation in
510 autumn-winter promoted NO_3^- attenuation lasting between 2 weeks and one month, while in
511 spring-summer the attenuation capacity remained for approximately three months (~16 L/s flow
512 rate). The isotopic characterization of the CW samples indicated that at least 60 % of the initial
513 NO_3^- was removed in the CW due to the induced denitrification. However, since in a few samples
514 NO_3^- was below the limit necessary for isotopic analysis, the contribution could have been higher.
515 The slope of $\delta^{18}\text{O}-\text{NO}_3^-$ versus $\delta^{15}\text{N}-\text{NO}_3^-$ obtained in the CW after the stubble application (1.0)
516 was close to that obtained in the experiments involving partially decomposed stubble incubated
517 at 24°C (1.1). Plant uptake seemed to play only a minor role in NO_3^- attenuation in the CW. The
518 treatment was considered safe because NO_2^- and NH_4^+ accumulation (below 0.2 and 0.1 mM,
519 respectively) decreased over time, surplus NPDOC (below 2.3 mM) released from the CW could
520 maintain NO_3^- attenuation downstream, and because the occurrence of BSR was discarded.
521 However, the longevity and effectivity of the treatment were limited due to the high O_2 content of
522 the inlet water, high water flow, and the possible generation of preferential flows within the CW.

523 **ACKNOWLEDGEMENTS**

524 This work was financed by the projects REMEDIATION (CGL2014-57215-C4), AGRO-SOS
525 (CGL2015-66016-R) and PACE-ISOTEC (CGL2017-87216-C4-1-R) financed by the Spanish

526 Government and AEI/FEDER financed by the European Union, and by MAG (2017 SGR 1733)
527 financed by the Catalan Government. R. Margalef-Marti thanks the Spanish Government for the
528 Ph.D. grant BES-2015-072882. D. Merchán was supported by the “Juan de la Cierva –
529 Formación” program (FJCI-2018-24920). We would also like to thank the CCiT of the Universitat
530 the Barcelona for the analytical support, and A. Fernández for his contribution to the study.

531 REFERENCES

- 532 91/676/EEC, 1991. Nitrates Directive. Council Directive 91/676/EEC of 12 December 1991,
533 concerning the protection of waters against pollution caused by nitrates from agricultural
534 sources. [WWW Document]. Off. J. Eur. Comm. URL
535 http://ec.europa.eu/environment/index_en.htm (accessed 4.9.17).
- 536 98/83/EC, 1998. Drinking Water Directive. Council Directive 98/83/EC, of 3 November 1998, on
537 the quality of water intended for human consumption. [WWW Document]. Off. J. Eur.
538 Comm. URL http://ec.europa.eu/environment/index_en.htm (accessed 4.9.17).
- 539 Akunna, J.C., Bizeau, C., Moletta, R., 1993. Nitrate and nitrite reductions with anaerobic sludge
540 using various carbon sources: Glucose, glycerol, acetic acid, lactic acid and methanol.
541 *Water Res.* 27, 1303–1312. [https://doi.org/10.1016/0043-1354\(93\)90217-6](https://doi.org/10.1016/0043-1354(93)90217-6)
- 542 Aravena, R., Robertson, W.D., 1998. Use of multiple isotope tracers to evaluate denitrification in
543 ground water: study of nitrate from a large-flux septic system plume. *Ground Water* 36,
544 975–982.
- 545 Bachand, P.A.M., Horne, A.J., 1999. Denitrification in constructed free-water surface wetlands:
546 I. Very high nitrate removal rates in a macrocosm study. *Ecol. Eng.* 14, 9–15.
547 [https://doi.org/10.1016/S0925-8574\(99\)00016-6](https://doi.org/10.1016/S0925-8574(99)00016-6)
- 548 Betlach, M.R., Tiedje, J.M., 1981. Kinetic Explanation for Accumulation of Nitrite, Nitric Oxide,
549 and Nitrous Oxide during Bacterial Denitrification. *Appl. Environ. Microbiol.* 42, 1074–
550 1084. <https://doi.org/Article>
- 551 Beutel, M.W., Newton, C.D., Brouillard, E.S., Watts, R.J., 2009. Nitrate removal in surface-flow
552 constructed wetlands treating dilute agricultural runoff in the lower Yakima Basin,

553 Washington. *Ecol. Eng.* 35, 1538–1546. <https://doi.org/10.1016/j.ecoleng.2009.07.005>

554 Böttcher, J., Strebel, O., Voerkelius, S., Schmidt, H.L., 1990. Using isotope fractionation of
555 nitrate-nitrogen and nitrate-oxygen for evaluation of microbial denitrification in a sandy
556 aquifer. *J. Hydrol.* 114, 413–424. [https://doi.org/10.1016/0022-1694\(90\)90068-9](https://doi.org/10.1016/0022-1694(90)90068-9)

557 Breulmann, M., Masyutenko, N.P., Kogut, B.M., Schroll, R., Dörfler, U., Buscot, F., Schulz, E.,
558 2014. Short-term bioavailability of carbon in soil organic matter fractions of different
559 particle sizes and densities in grassland ecosystems. *Sci. Total Environ.* 497–498, 29–37.
560 <https://doi.org/10.1016/j.scitotenv.2014.07.080>

561 Carrey, R., Otero, N., Vidal-Gavilan, G., Ayora, C., Soler, A., Gómez-Alday, J.J., 2014. Induced
562 nitrate attenuation by glucose in groundwater: Flow-through experiment. *Chem. Geol.* 370,
563 19–28. <https://doi.org/10.1016/j.chemgeo.2014.01.016>

564 Carrey, R., Rodríguez-Escales, P., Soler, A., Otero, N., 2018. Tracing the role of endogenous
565 carbon in denitrification using wine industry by-product as an external electron donor:
566 Coupling isotopic tools with mathematical modeling. *J. Environ. Manage.* 207, 105–115.
567 <https://doi.org/10.1016/j.jenvman.2017.10.063>

568 Christensen, P.B., Srensen, J.A.N., 1986. Temporal Variation of Denitrification Activity in Plant-
569 Covered , Littoral Sediment from Lake Hampen , Denmark 51, 1174–1179.

570 Cooper, A.B., Cooke, J.G., 1984. Nitrate loss and transformation in 2 vegetated headwater
571 streams. *New Zeal. J. Mar. Freshw. Res.* 18, 441–450.
572 <https://doi.org/10.1080/00288330.1984.9516065>

573 Coplen, T.B., 2011. Guidelines and recommended terms for expression of stable-isotope-ratio
574 and gas-ratio measurement results. *Rapid Commun. Mass Spectrom.* 25, 2538–2560.
575 <https://doi.org/10.1002/rcm.5129>

576 Dawson, R.N., Murphy, K.L., 1972. The temperature dependency of biological denitrification.
577 *Water Res.* 6, 71–83. [https://doi.org/10.1016/0043-1354\(72\)90174-1](https://doi.org/10.1016/0043-1354(72)90174-1)

578 Dogramaci, S., Herczeg, A., Schiff, S., Bone, Y., 2001. Controls on $\delta^{34}\text{S}$ and $\delta^{18}\text{O}$ of dissolved
579 sulfate in aquifers of the Murray Basin, Australia and their use as indicators of flow

580 processes. *Appl. Geochemistry* 16, 475–488. <https://doi.org/10.1016/S0883->
581 2927(00)00052-4

582 Estrada, N.L., Böhlke, J.K., Sturchio, N.C., Gu, B., Harvey, G., Burkey, K.O., Grantz, D.A.,
583 McGrath, M.T., Anderson, T.A., Rao, B., Sevanthi, R., Hatzinger, P.B., Jackson, W.A.,
584 2017. Stable isotopic composition of perchlorate and nitrate accumulated in plants:
585 Hydroponic experiments and field data. *Sci. Total Environ.* 595, 556–566.
586 <https://doi.org/10.1016/j.scitotenv.2017.03.223>

587 Fukada, T., Hiscock, K.M., Dennis, P.F., Grischek, T., 2003. A dual isotope approach to identify
588 denitrification in groundwater at a river-bank infiltration site. *Water Res.* 37, 3070–3078.
589 [https://doi.org/10.1016/S0043-1354\(03\)00176-3](https://doi.org/10.1016/S0043-1354(03)00176-3)

590 Ge, S., Peng, Y., Wang, S., Lu, C., Cao, X., Zhu, Y., 2012. Nitrite accumulation under constant
591 temperature in anoxic denitrification process: The effects of carbon sources and
592 COD/NO₃-N. *Bioresour. Technol.* 114, 137–143.
593 <https://doi.org/10.1016/j.biortech.2012.03.016>

594 Giles, M., Morley, N., Baggs, E.M., Daniell, T.J., 2012. Soil nitrate reducing processes - Drivers,
595 mechanisms for spatial variation, and significance for nitrous oxide production. *Front.*
596 *Microbiol.* 3, 1–16. <https://doi.org/10.3389/fmicb.2012.00407>

597 Grau-Martínez, A., Torrentó, C., Carrey, R., Rodríguez-Escales, P., Domènech, C., Ghiglieri, G.,
598 Soler, A., Otero, N., 2017. Feasibility of two low-cost organic substrates for inducing
599 denitrification in artificial recharge ponds: Batch and flow-through experiments. *J. Contam.*
600 *Hydrol.* 198, 48–58. <https://doi.org/10.1016/j.jconhyd.2017.01.001>

601 Gumbricht, T., 1993. Nutrient removal capacity in submersed macrophyte pond systems in a
602 temperature climate. *Ecol. Eng.* 2, 49–61. [https://doi.org/10.1016/0925-8574\(93\)90026-C](https://doi.org/10.1016/0925-8574(93)90026-C)

603 Ilyas, H., Masih, I., 2017. The performance of the intensified constructed wetlands for organic
604 matter and nitrogen removal: A review. *J. Environ. Manage.* 198, 372–383.
605 <https://doi.org/10.1016/j.jenvman.2017.04.098>

606 Jacobs, A.E., Harrison, J.A., 2014. Effects of floating vegetation on denitrification, nitrogen

607 retention, and greenhouse gas production in wetland microcosms. *Biogeochemistry* 119,
608 51–66. <https://doi.org/10.1007/s10533-013-9947-9>

609 Kang, Y., Zhang, J., Li, B., Zhang, Y., Sun, H., Hao Ngo, H., Guo, W., Xie, H., Hu, Z., Zhao, C.,
610 2018. Improvement of bioavailable carbon source and microbial structure toward
611 enhanced nitrate removal by *Tubifex tubifex*. *Chem. Eng. J.* 353, 699–707.
612 <https://doi.org/10.1016/j.cej.2018.07.182>

613 Kelso, B.H.L., Smith, R. V., Laughlin, R.J., Lennox, S.D., 1997. Dissimilatory nitrate reduction in
614 anaerobic sediments leading to river nitrite accumulation. *Appl. Environ. Microbiol.* 63,
615 4679–4685.

616 Knowles, R., 1982. Denitrification. *Microbiol. Rev.* 46, 43–70.

617 Kong, L., Wang, Y. Bin, Zhao, L.N., Chen, Z.H., 2009. Enzyme and root activities in surface-flow
618 constructed wetlands. *Chemosphere* 76, 601–608.
619 <https://doi.org/10.1016/j.chemosphere.2009.04.056>

620 Kovacic, D.A., David, M.B., Gentry, L.E., Starks, K.M., Cooke, R.A., 2000. Effectiveness of
621 Constructed Wetlands in Reducing Nitrogen and Phosphorus Export from Agricultural Tile
622 Drainage. *J. Environ. Qual.* 29, 1262.
623 <https://doi.org/10.2134/jeq2000.00472425002900040033x>

624 Kraft, B., Tegetmeyer, H.E., Sharma, R., Klotz, M.G., Ferdelman, T.G., Hettich, R.L., Geelhoed,
625 J.S., Strous, M., 2014. The environmental controls that govern the end product of bacterial
626 nitrate respiration. *Science* (80). 345, 3–7.

627 Laverman, A.M., Pallud, C., Abell, J., Cappellen, P. Van, 2012. Comparative survey of potential
628 nitrate and sulfate reduction rates in aquatic sediments. *Geochim. Cosmochim. Acta* 77,
629 474–488. <https://doi.org/10.1016/j.gca.2011.10.033>

630 Lin, Y.F., Jing, S.R., Wang, T.W., Lee, D.Y., 2002. Effects of macrophytes and external carbon
631 sources on nitrate removal from groundwater in constructed wetlands. *Environ. Pollut.*
632 119, 413–420. [https://doi.org/10.1016/S0269-7491\(01\)00299-8](https://doi.org/10.1016/S0269-7491(01)00299-8)

633 Lu, S., Hu, H., Sun, Y., Yang, J., 2009. Effect of carbon source on the denitrification in

634 constructed wetlands. *J. Environ. Sci.* 21, 1036–1043. <https://doi.org/10.1016/S1001->
635 0742(08)62379-7

636 Lund, L., Horne, A., Williams, A., 1999. Estimating denitrification in a large constructed
637 wetland using stable nitrogen isotope ratios. *Ecol. Eng.* 14, 67–76.
638 [https://doi.org/10.1016/S0925-8574\(99\)00020-8](https://doi.org/10.1016/S0925-8574(99)00020-8)

639 Margalef-Marti, R., Carrey, R., Soler, A., Otero, N., 2019. Evaluating the potential use of a dairy
640 industry residue to induce denitrification in polluted water bodies: A flow-through
641 experiment. *J. Environ. Manage.* 245. <https://doi.org/10.1016/j.jenvman.2019.03.086>

642 Mariotti, A., Germon, J.C., Hubert, P., Kaiser, P., Letolle, R., Tardieux, A., Tardieux, P., 1981.
643 Experimental determination of nitrogen kinetic isotope fractionation: Some principles;
644 illustration for the denitrification and nitrification processes. *Plant Soil* 62, 413–430.
645 <https://doi.org/10.1007/BF02374138>

646 Mariotti, A., Landreau, A., Simon, B., 1988. ¹⁵N isotope biogeochemistry and natural
647 denitrification process in groundwater: Application to the chalk aquifer of northern France.
648 *Geochim. Cosmochim. Acta* 52, 1869–1878. [https://doi.org/10.1016/0016-7037\(88\)90010-](https://doi.org/10.1016/0016-7037(88)90010-5)
649 5

650 McIlvin, M.R., Altabet, M.A., 2005. Chemical conversion of nitrate and nitrite to nitrous oxide for
651 nitrogen and oxygen isotopic analysis in freshwater and seawater. *Anal Chem* 77, 5589–
652 5595. <https://doi.org/10.1021/ac050528s>

653 Merchán, D., Causapé, J., Abrahão, R., 2013. Impact of irrigation implementation on hydrology
654 and water quality in a small agricultural basin in Spain. *Hydrol. Sci. J.* 58, 1400–1413.
655 <https://doi.org/10.1080/02626667.2013.829576>

656 Merchán, D., Causapé, J., Abrahão, R., García-Garizábal, I., 2015. Assessment of a newly
657 implemented irrigated area (Lerma Basin, Spain) over a 10-year period. II: Salts and
658 nitrate exported. *Agric. Water Manag.* <https://doi.org/10.1016/j.agwat.2015.04.019>

659 Merchán, D., Otero, N., Soler, A., Causapé, J., 2014. Main sources and processes affecting
660 dissolved sulphates and nitrates in a small irrigated basin (Lerma Basin, Zaragoza, Spain):

661 Isotopic characterization. *Agric. Ecosyst. Environ.* 195, 127–138.
662 <https://doi.org/10.1016/j.agee.2014.05.011>

663 Peralta, A.L., Matthews, J.W., Flanagan, D.N., Kent, A.D., 2012. Environmental factors at
664 dissimilar spatial scales influence plant and microbial communities in restored wetlands.
665 *Wetlands* 32, 1125–1134. <https://doi.org/10.1007/s13157-012-0343-3>

666 Rivett, M.O., Buss, S.R., Morgan, P., Smith, J.W.N., Bemment, C.D., 2008. Nitrate attenuation
667 in groundwater: A review of biogeochemical controlling processes. *Water Res.* 42, 4215–
668 4232. <https://doi.org/10.1016/j.watres.2008.07.020>

669 Rogers, K.H., Breen, P.F., Chick, A.J., 1991. Nitrogen Removal in Experimental Wetland
670 Treatment Systems: Evidence for the Role of Aquatic Plants. *Res. J. Water Pollut. Control*
671 *Fed.* 63, 934–941.

672 Ryabenko, E., Altabet, M. a., Wallace, D.W.R., 2009. Effect of chloride on the chemical
673 conversion of nitrate to nitrous oxide for $\delta^{15}\text{N}$ analysis. *Limnol. Oceanogr. Methods* 7,
674 545–552. <https://doi.org/10.4319/lom.2009.7.545>

675 Scott, J.T., McCarthy, M.J., Gardner, W.S., Doyle, R.D., 2008. Denitrification, dissimilatory
676 nitrate reduction to ammonium, and nitrogen fixation along a nitrate concentration gradient
677 in a created freshwater wetland. *Biogeochemistry* 87, 99–111.
678 <https://doi.org/10.1007/s10533-007-9171-6>

679 Si, Z., Song, X., Wang, Y., Cao, X., Zhao, Y., Wang, B., Chen, Y., Arefe, A., 2018. Intensified
680 heterotrophic denitrification in constructed wetlands using four solid carbon sources:
681 Denitrification efficiency and bacterial community structure. *Bioresour. Technol.* 267, 416–
682 425. <https://doi.org/10.1016/j.biortech.2018.07.029>

683 Sirivedhin, T., Gray, K.A., 2006. Factors affecting denitrification rates in experimental wetlands:
684 Field and laboratory studies. *Ecol. Eng.* 26, 167–181.
685 <https://doi.org/10.1016/j.ecoleng.2005.09.001>

686 Soana, E., Balestrini, R., Vincenzi, F., Bartoli, M., Castaldelli, G., 2017. Mitigation of nitrogen
687 pollution in vegetated ditches fed by nitrate-rich spring waters. *Agric. Ecosyst. Environ.*

688 243, 74–82. <https://doi.org/10.1016/j.agee.2017.04.004>

689 Sobczak, W. V., Findlay, S., 2002. Variation in Bioavailability of Dissolved Organic Carbon
690 among Stream Hyporheic Flowpaths. *Ecology* 83, 3194–3209.

691 Søvik, A.K., Mørkved, P.T., 2008. Use of stable nitrogen isotope fractionation to estimate
692 denitrification in small constructed wetlands treating agricultural runoff. *Sci. Total Environ.*
693 392, 157–165. <https://doi.org/10.1016/j.scitotenv.2007.11.014>

694 Spieles, D.J., Mitsch, W.J., 1999. The effects of season and hydrologic and chemical loading on
695 nitrate retention in constructed wetlands: A comparison of low- and high-nutrient riverine
696 systems. *Ecol. Eng.* 14, 77–91. [https://doi.org/10.1016/S0925-8574\(99\)00021-X](https://doi.org/10.1016/S0925-8574(99)00021-X)

697 Spoelstra, J., Schiff, S.L., Semkin, R.G., Jeffries, D.S., Elgood, R.J., 2010. Nitrate attenuation in
698 a small temperate wetland following forest harvest. *For. Ecol. Manage.* 259, 2333–2341.
699 <https://doi.org/10.1016/j.foreco.2010.03.006>

700 Strebel, O., Böttcher, J., Fritz, P., 1990. Use of isotope fractionation of sulfate-sulfur and sulfate-
701 oxygen to assess bacterial desulfurification in a sandy aquifer. *J. Hydrol.* 121, 155–172.
702 [https://doi.org/10.1016/0022-1694\(90\)90230-U](https://doi.org/10.1016/0022-1694(90)90230-U)

703 Tanner, C.C., Nguyen, M.L., Sukias, J.P.S., 2005. Nutrient removal by a constructed wetland
704 treating subsurface drainage from grazed dairy pasture. *Agric. Ecosyst. Environ.* 105,
705 145–162. <https://doi.org/10.1016/j.agee.2004.05.008>

706 Trois, C., Coulon, F., de Combret, C.P., Martins, J.M.F., Oxarango, L., 2010. Effect of pine bark
707 and compost on the biological denitrification process of non-hazardous landfill leachate:
708 Focus on the microbiology. *J. Hazard. Mater.* 181, 1163–1169.
709 <https://doi.org/10.1016/j.jhazmat.2010.05.077>

710 Uusheimo, S., Tulonen, T., Aalto, S.L., Arvola, L., 2018. Mitigating agricultural nitrogen load with
711 constructed ponds in northern latitudes: A field study on sedimental denitrification rates.
712 *Agric. Ecosyst. Environ.* 261, 71–79. <https://doi.org/10.1016/j.agee.2018.04.002>

713 Vidal-Gavilan, G., Folch, A., Otero, N., Solanas, A.M., Soler, A., 2013. Isotope characterization
714 of an in situ biodenitrification pilot-test in a fractured aquifer. *Appl. Geochemistry* 32, 153–

715 163. <https://doi.org/10.1016/j.apgeochem.2012.10.033>

716 Vitousek, P.M., Aber, J.D., Howarth, R.W., Likens, G.E., Matson, P.A., Schindler, D.W.,
717 Schlesinger, W.H., Tilman, D.G., 1997. Summary for Policymakers, in: Intergovernmental
718 Panel on Climate Change (Ed.), *Climate Change 2013 - The Physical Science Basis*.
719 Cambridge University Press, Cambridge, pp. 1–30.
720 <https://doi.org/10.1017/CBO9781107415324.004>

721 Vymazal, J., 2007. Removal of nutrients in various types of constructed wetlands. *Sci. Total*
722 *Environ.* 380, 48–65. <https://doi.org/10.1016/j.scitotenv.2006.09.014>

723 Ward, M.H., DeKok, T.M., Levallois, P., Brender, J., Gulis, G., Nolan, B.T., VanDerslice, J.,
724 2005. Workgroup Report: Drinking-Water Nitrate and Health—Recent Findings and
725 Research Needs. *Environ. Health Perspect.* 113, 1607–1614.
726 <https://doi.org/10.1289/ehp.8043>

727 Warneke, S., Schipper, L.A., Matiasek, M.G., Scow, K.M., Cameron, S., Bruesewitz, D.A.,
728 McDonald, I.R., 2011. Nitrate removal, communities of denitrifiers and adverse effects in
729 different carbon substrates for use in denitrification beds. *Water Res.* 45, 5463–5475.
730 <https://doi.org/10.1016/j.watres.2011.08.007>

731 Wu, H., Zhang, J., Ngo, H.H., Guo, W., Hu, Z., Liang, S., Fan, J., Liu, H., 2015. A review on the
732 sustainability of constructed wetlands for wastewater treatment: Design and operation.
733 *Bioresour. Technol.* 175, 594–601. <https://doi.org/10.1016/j.biortech.2014.10.068>

734

Figure 1. CW design. Photograph of the surface flow CW with emergent macrophytes. The sampling points are depicted by white squares (H1 to H6), and the water flow within the CW with striped arrows. Non-treated water flow discharging to the Lerma gully is depicted with black arrows, and that of treated water with a white arrow.

Figure 2. Evolution of denitrification in the biostimulated microcosms. NO_3^- (circles joined by a continuous line) and NO_2^- (squares joined by a dashed line) measured in (A) the batch experiments employing different C sources and (B) the experiments testing the effects of temperature and lifespan of the stubble.

Figure 3. NO_3^- -O and NO_3^- -N isotopic fractionation throughout denitrification in the biostimulated microcosms. Results from the batch experiments testing (A, B) different C sources and (C, D) the effects of temperature and lifespan of the stubble.

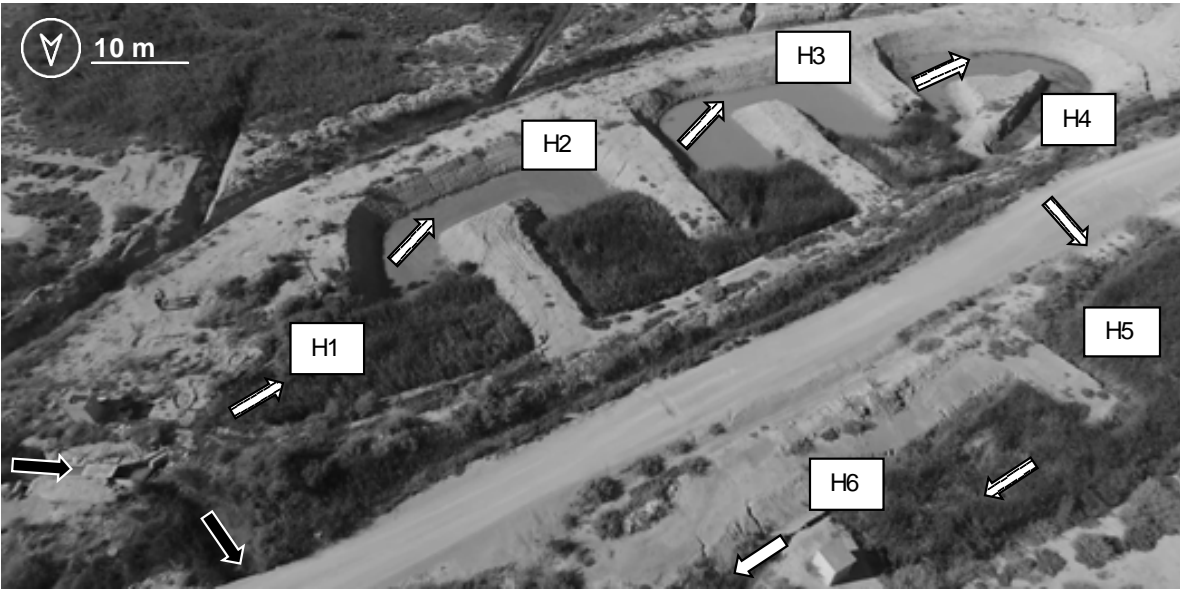
Figure 4. NO_3^- attenuation in the CW before the application of stubble. Black circles depict the sampling campaigns performed at a ~5.5 L/s flow rate (full symbols for the campaign of June 14, 2017 and empty symbols for that of September 5, 2017), and grey circles depict the sampling campaigns performed at a ~2.5 L/s flow rate (September 12, 2017). (A) NO_3^- concentration along the CW flow direction, where dashed lines represent the range of NO_3^- concentrations measured at the inlet of the CW throughout the study period. (B) Isotopic characterization including the regression line, where the dashed square represents the range of isotopic compositions measured at the inlet of the CW throughout the study period.

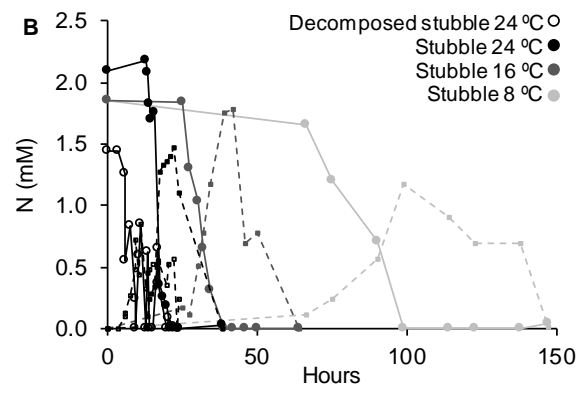
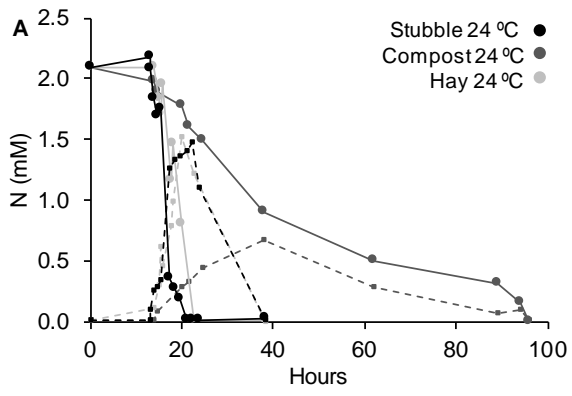
Figure 5. NO_3^- attenuation in the CW after the first application of stubble in autumn. (A) NO_3^- concentration along the CW, where dashed lines represent the range of NO_3^- concentrations measured at the inlet of the CW throughout the study period. Full symbols depict the sampling campaign conducted on October 2, 2017, and empty symbols depict that conducted on October 10, 2017 (seven and fourteen days after the application of the stubble, respectively). (B, C) NO_3^- concentrations monitored at the inlet (black) and outlet (grey) in the days before and after the sampling campaigns, respectively.

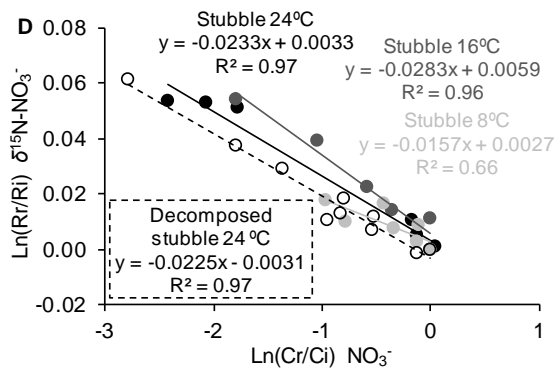
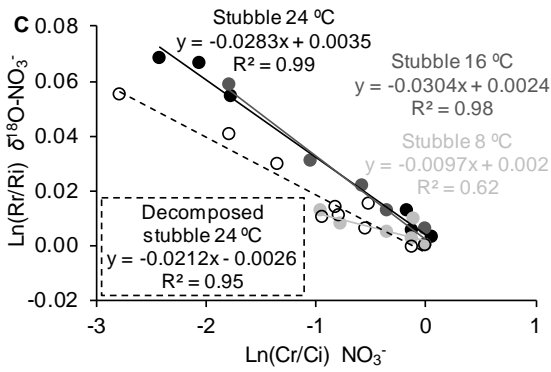
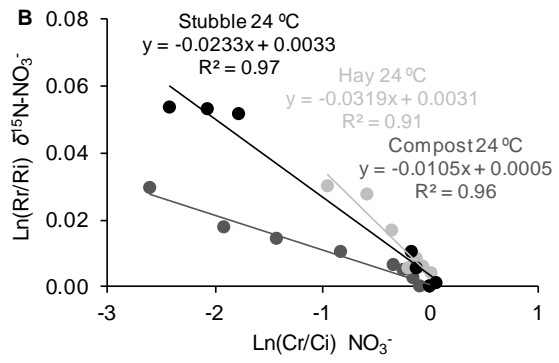
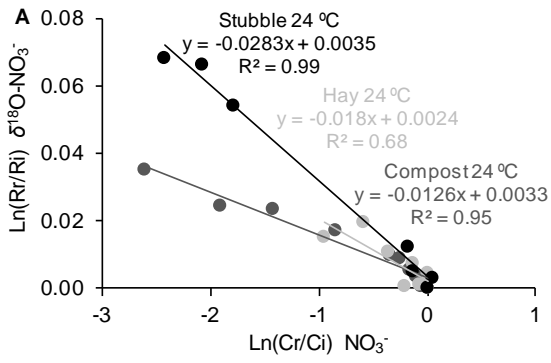
Figure 6. NO_3^- attenuation in the CW after the second application of stubble in spring. (A) NO_3^- concentrations monitored at the inlet (black) and outlet (grey) of the CW throughout the first days of treatment. (B) NO_3^- concentrations along the CW flow direction, for each sampling campaign. Dashed lines represent the range of NO_3^- concentrations measured at the inlet of the CW throughout the study period. The 7 sampling campaigns performed throughout the 100 days after stubble application are represented by shades of grey (from darker to lighter as time progressed), with the last represented by the empty symbols. The campaign performed before application is represented by asterisks.

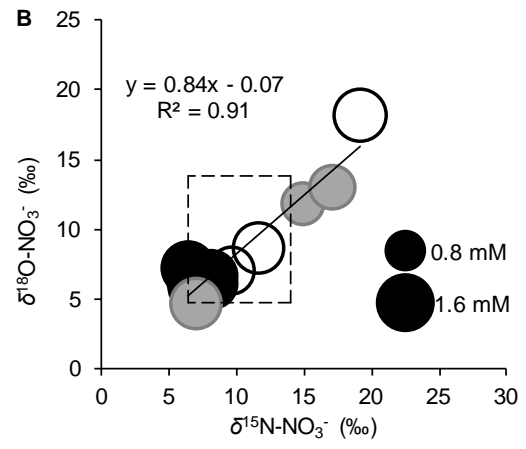
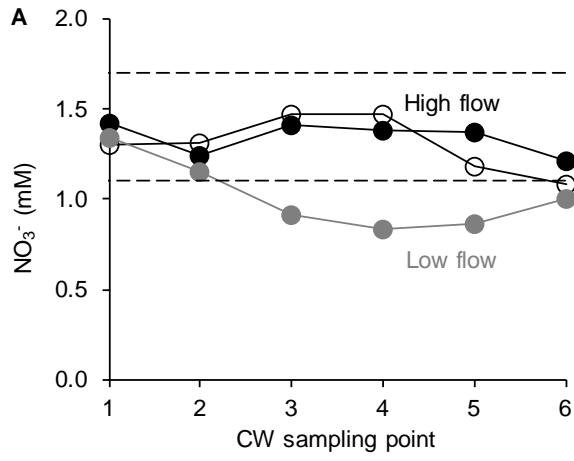
Figure 7. Denitrification efficiency in the CW determined from the laboratory-obtained ϵ values. Isotopic values obtained from the samples collected at the CW, including the regression line (black). The three denitrification % lines (grey) presented correspond to the three conditions tested in the laboratory that were closest to the CW conditions throughout the field-scale test.

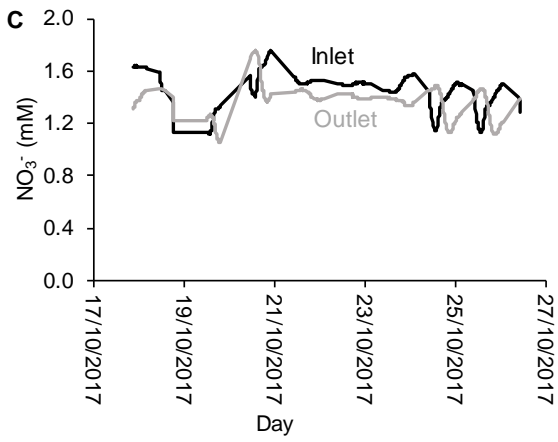
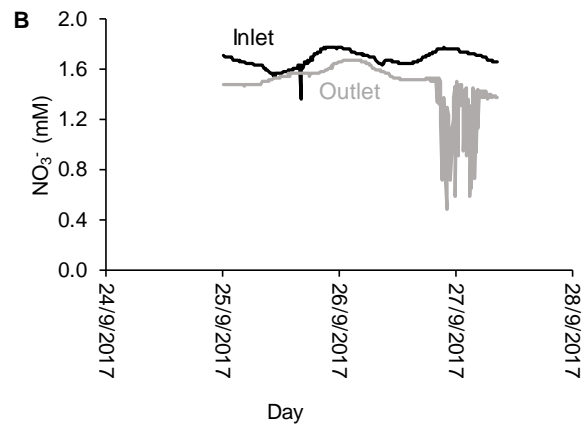
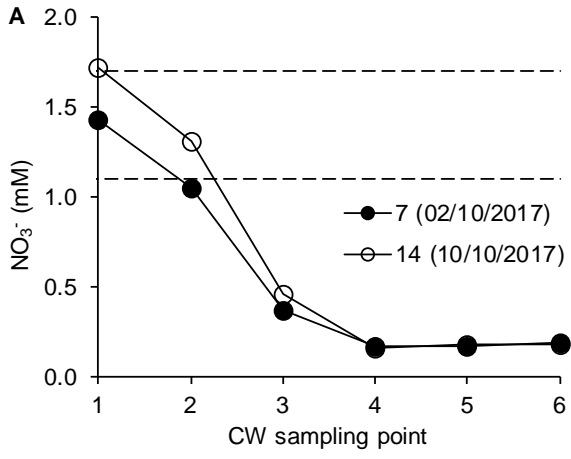
Figure 8. Dissolved organic C in the CW before and after application of stubble. NPDOC concentration along the CW flow. The 5 sampling campaigns conducted within the 63 days after stubble application are presented in shades of grey, from darkest to lightest as time progressed. The campaign performed before application is represented by asterisks.

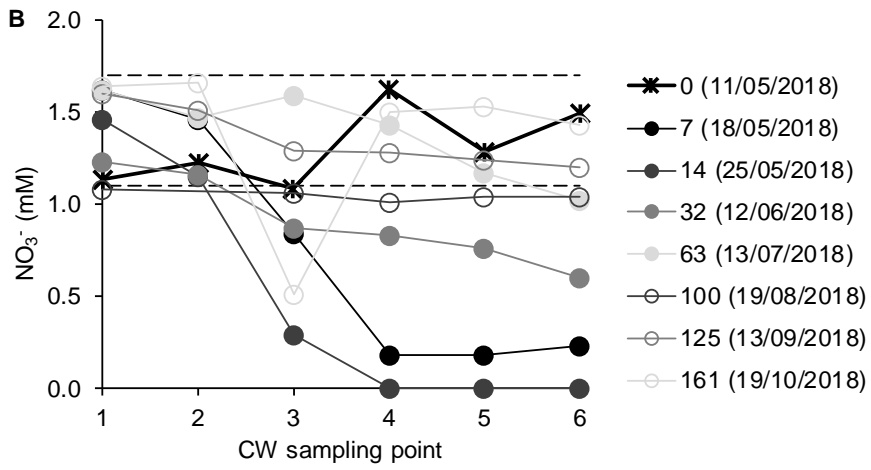
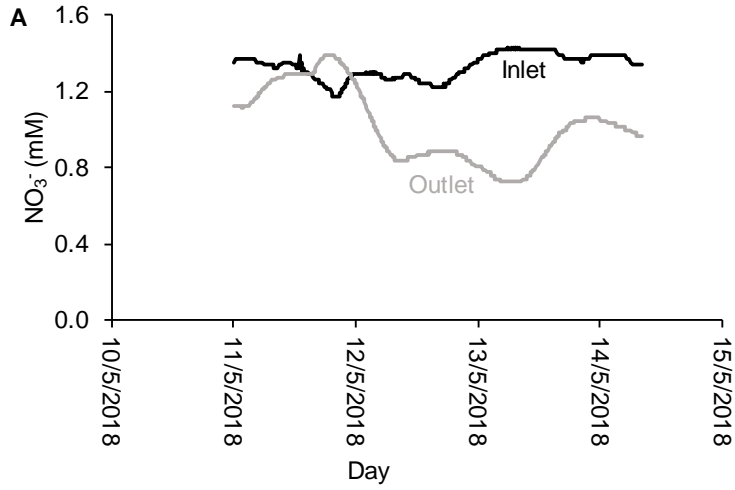


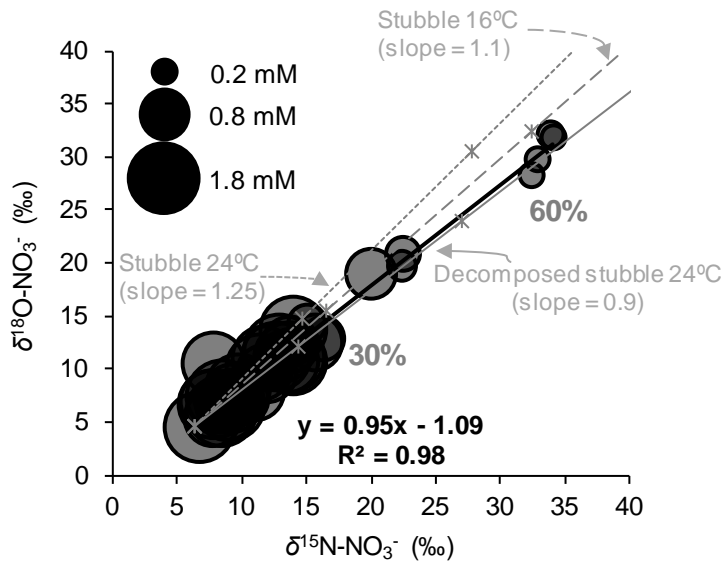












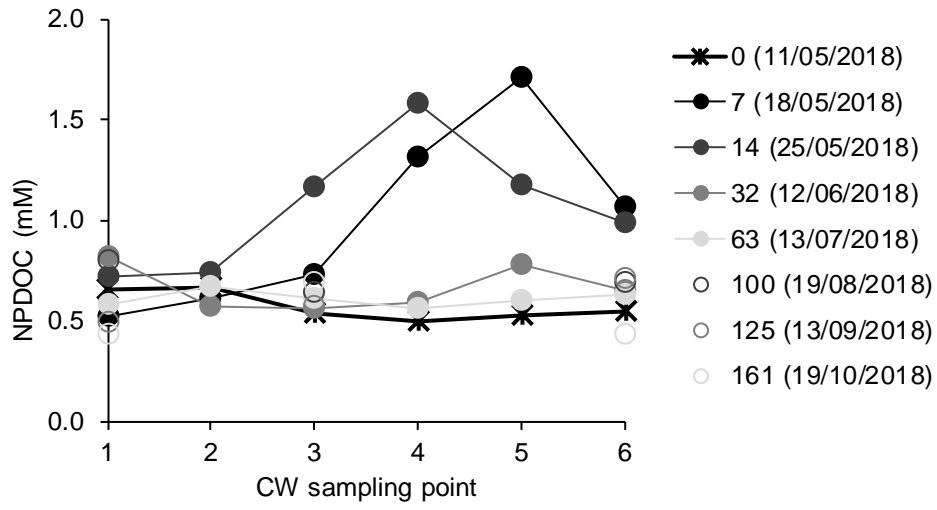


Table 1. Series of experiments. Tested conditions and composition of microcosms. DIW = deionized water.

Series	Condition	Code	C source	Material (g)	C (g/L)	Water source (100 mL)	Temperature (°C)
I	Biostimulated	C-24	Animal compost	0.25	0.8	Wetland	24
	Control	C-24-blank	Animal compost	0.25	0.8	DIW	24
II	Biostimulated	H-24	Wheat hay	1	4.2	Wetland	24
	Control	H-24-blank	Wheat hay	1	4.2	DIW	24
III	Biostimulated	S-24	Corn stubble	1	3.6	Wetland	24
	Control	S-24-blank	Corn stubble	1	3.6	DIW	24
IV	Biostimulated	S-16	Corn stubble	1	3.6	Wetland	16
	Control	S-16-blank	Corn stubble	1	3.6	DIW	16
V	Biostimulated	S-8	Corn stubble	1	3.6	Wetland	8
	Control	S-8-blank	Corn stubble	1	3.6	DIW	8
VI	Biostimulated	DS-24	Decomposed stubble	1	3.6	Wetland	24
	Control	DS-24-blank	Decomposed stubble	1	3.6	DIW	24

Table 2. Sampling campaigns. Sampling dates and operation mode of the CW for all sampling campaigns (six samples each).

Test period	Date	Days since stubble addition	Operation mode	Observations
I	14/06/2017	-	High flow	No external organic C addition
	05/09/2017	-	High flow	
	12/09/2017	-	Low flow	
II	02/10/2017	7	High flow	First organic C source addition on 25/09/2017
	10/10/2017	14		
III	11/05/2018	0	High flow	Second organic C source addition on 11/05/2018
	18/05/2018	7		
	25/05/2018	14		
	12/06/2018	32		
	13/07/2018	63		
	19/08/2018	100		
	13/09/2018	125		
	19/10/2018	161		

Table 3. Waste products composition. C and N concentrations and isotopic composition of the corn stubble, wheat hay, and animal compost employed to promote denitrification.

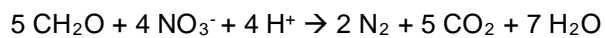
SOURCE	C (%)	N (%)	$\delta^{13}\text{C}$ (‰)	$\delta^{15}\text{N}$ (‰)
Animal compost	32.1	3.1	-25.4	10.8
Wheat hay	40.9	0.4	-27.8	3.0
Corn stubble	36.1	1.0	-13.6	6.7

Table 4. Calculated ϵ values from the laboratory microcosms. $\epsilon^{18}\text{O}_{\text{NO}_3/\text{N}_2}$, $\epsilon^{15}\text{N}_{\text{NO}_3/\text{N}_2}$, and $\epsilon^{15}\text{N}_{\text{NO}_3/\text{N}_2}/\epsilon^{18}\text{O}_{\text{NO}_3/\text{N}_2}$ for each condition tested at laboratory-scale.

EXPERIMENT	$\epsilon^{18}\text{O}_{\text{NO}_3/\text{N}_2}$	$\epsilon^{15}\text{N}_{\text{NO}_3/\text{N}_2}$	$\epsilon^{15}\text{N}/\epsilon^{18}\text{O}$
Compost 24°C	-12.6	-10.5	0.8
Hay 24°C	-18.0	-31.9	1.8
Stubble 24°C	-28.3	-23.3	0.8
Stubble 16°C	-30.4	-28.3	0.9
Stubble 8°C	-9.7	-15.7	1.6
Decomposed stubble 24°C	-21.2	-22.5	1.1

Supporting Information, section S1: $\delta^{13}\text{C}$ -DIC results

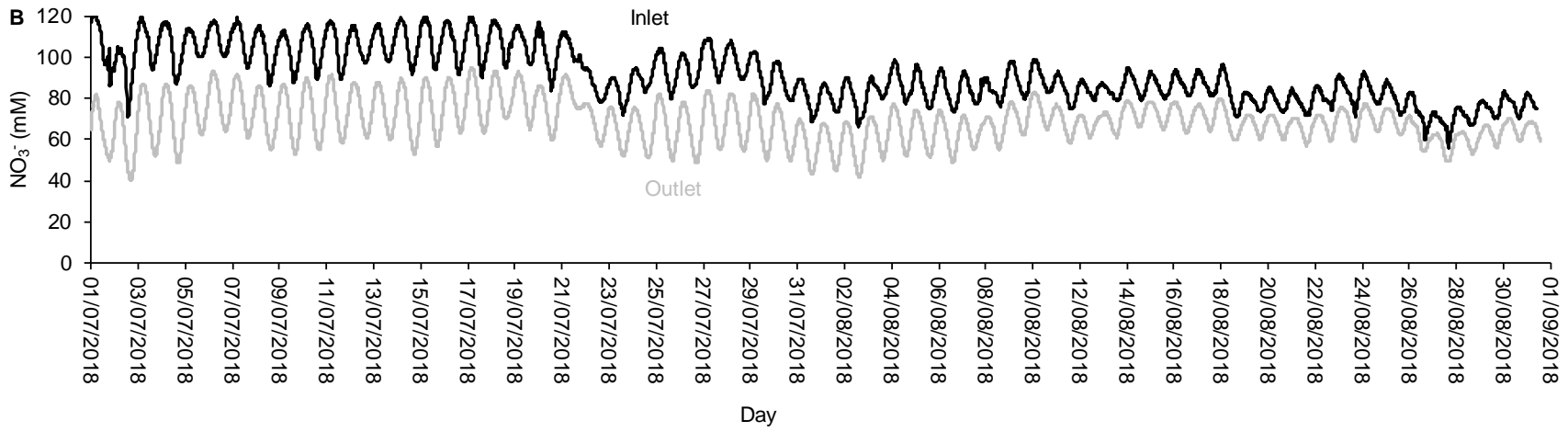
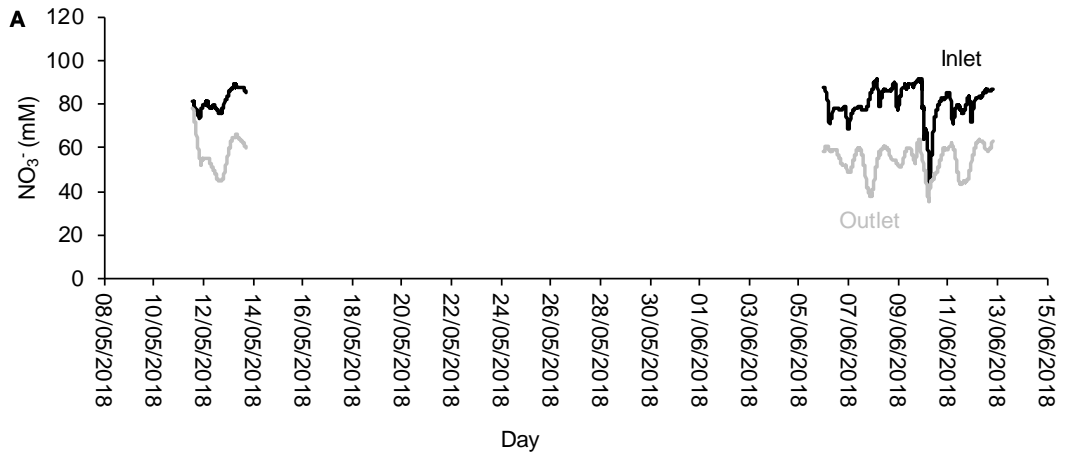
The $\delta^{13}\text{C}$ -DIC results provided information about the transformation of organic C from the waste materials to inorganic C (**Equation S1**). These results are presented in Supporting Information **Table S2**. As DIC concentration increased, the initial $\delta^{13}\text{C}$ -DIC in water of -13.1 ‰ decreased to -15.5 ‰ and -20.0 ‰ in the microcosms containing hay and compost, respectively, but remained unchanged in the stubble experiment (**Figure S2**). The flat trend observed in the experiments with stubble, in contrast to the correlations obtained with the experiments employing hay and compost, was attributed to the intrinsic $\delta^{13}\text{C}$ -C_{bulk} of each material (**Table 3**). The most significant change in the $\delta^{13}\text{C}$ -DIC was observed for the experiment involving hay, which presented a lower $\delta^{13}\text{C}$ -C_{bulk} (-27.8 ‰) compared to that of compost (-25.4‰); stubble did not produce any change because its $\delta^{13}\text{C}$ -C_{bulk} (-13.6 ‰) is close to the $\delta^{13}\text{C}$ -DIC of water (-13.1 ‰). Hay and stubble presented a different intrinsic $\delta^{13}\text{C}$ -C_{bulk} as they are classified as C4 and C3 plants, respectively (Leary, 1988). An isotopic fractionation effect derived from the bacterial C metabolism did not seem to be significant under the tested conditions. These results show that the $\delta^{13}\text{C}$ -DIC analysis can be applied to assess the efficiency of biostimulation strategies at field-scale when C sources with an intrinsic $\delta^{13}\text{C}$ -C_{bulk} differing from the $\delta^{13}\text{C}$ -DIC of water (such as C4 plant materials) are used.



Equation S1

References:

Leary, M.H.O., 1988. Carbon Isotopes in Photosynthesis. *Bioscience* 38, 328–336.



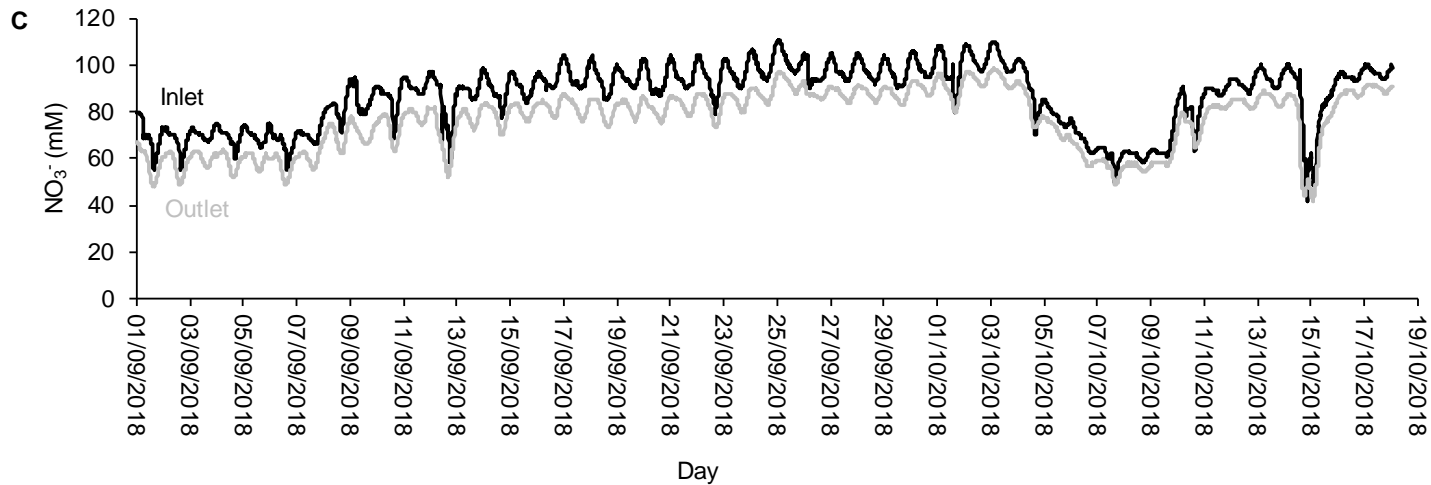


Figure S1. Monitored NO₃⁻ concentrations at the inlet and outlet of the CW during the third period of the test. The NO₃⁻ retention time in the CW was considered for the outlet data. (A) May-June 2018, (B) July-August 2018 and (C) September-October 2018. The data between 10/05/2018 and 06/06/2018 and between 13/06/2018 and 01/07/2018 is lacking due to technical issues.

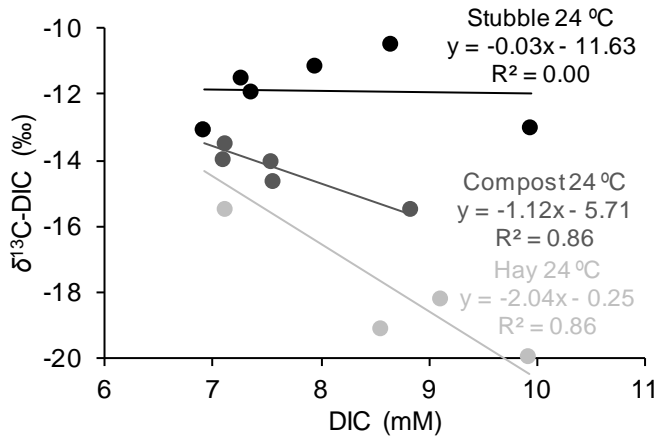


Figure S2. Relationship between $\delta^{13}\text{C-DIC}$ and DIC concentration throughout denitrification.

Correlation between $\delta^{13}\text{C-DIC}$ and DIC concentration in the samples collected from laboratory batch experiments testing different C sources for the induction of the bacterial NO_3^- reduction.

Table S1. Precipitation and temperature records. Data collected from a meteorological station near the CW (coordinates X = 649168.18 and Y = 4662201.55).

Month	Precipitation (mm)	Average temperature (°C)	Minimum temperature (°C)	Maximum temperature (°C)
June-17	80.2	23.2	13.2	30.2
July-17	46.6	23.6	15.1	28.3
August-17	79.4	23.2	16.5	29.1
September-17	47.2	17.6	12.5	23.3
October-17	11.1	16.0	10.3	20.4
November-17	13.1	8.6	2.5	15.3
December-17	17.3	5.1	0.3	9.4
January-18	64.5	6.8	2.0	12.7
February-18	37.6	4.9	0.9	10.0
March-18	82.8	8.5	3.8	12.3
April-18	173.9	12.8	5.8	16.8
May-18	54.7	15.8	9.6	20.0
June-18	17.3	20.9	15.8	26.2
July-18	44.2	24.6	19.9	28.4
August-18	4.4	23.8	19.1	28.2
September-18	19.7	21.2	15.9	23.9
October-18	0.0	16.3	13.1	18.8

Table S2. Standards for isotopic analysis. International and laboratory (CCiT) standards used for normalization of the results.

Analysis	Standards
$\delta^{15}\text{N-NO}_3^-$	USGS-32, USGS-34, USGS-35 and CCiT-IWS ($\delta^{15}\text{N} = +16.9 \text{ ‰}$)
$\delta^{18}\text{O-NO}_3^-$	USGS-32, USGS-34, USGS-35 and CCiT-IWS ($\delta^{18}\text{O} = +28.5 \text{ ‰}$)
$\delta^{15}\text{N-N}_{\text{bulk}}$	USGS-40, IAEA-N1, IAEA-NO3, IAEA-N2
$\delta^{13}\text{C-C}_{\text{bulk}}$	USGS-40, IAEA-CH7, IAEA-CH6
$\delta^{13}\text{C-DIC}$	CCiT- NaHCO_3 ($\delta^{13}\text{C} = -4.4 \text{ ‰}$), CCiT- NaKHCO_3 ($\delta^{13}\text{C} = -18.7 \text{ ‰}$) and CCiT- KHCO_3 ($\delta^{13}\text{C} = +29.2 \text{ ‰}$)
$\delta^{34}\text{S-SO}_4^{2-}$	NBS-127, SO5, SO6 and CCiT-YCEM ($\delta^{34}\text{S} = +12.8 \text{ ‰}$)
$\delta^{18}\text{O-SO}_4^{2-}$	NBS-127, SO6, USGS-34, CCiT-YCEM ($\delta^{18}\text{O} = +17.6 \text{ ‰}$) and CCiT-ACID ($\delta^{18}\text{O} = +13.2 \text{ ‰}$)

Table S3. Batch experiments results. N and C compounds concentration and isotopic composition.

Code	Hour	NO ₃ ⁻ (mM)	NO ₂ ⁻ (mM)	NH ₄ ⁺ (mM)	N ₂ O (nmol)	N ₂ O (%) [*]	NPDOC (mM)	DIC (mM)	δ ¹⁵ N-NO ₃ ⁻ (‰)	δ ¹⁸ O-NO ₃ ⁻ (‰)	δ ¹³ C-DIC (‰)
CW water	0.0	2.1	0.0	0.0	n.d.	n.d.	0.5	6.9	6.4	4.9	-13.1
C-24-1	14.0	2.0	0.0	0.1	n.d.	n.d.	10.2	7.1	4.6	5.7	-13.5
C-24-2	14.5	1.9	0.1	0.1	n.d.	n.d.	n.d.	n.d.	6.7	8.5	n.d.
C-24-3	20.0	1.8	0.3	0.1	n.d.	n.d.	9.0	7.1	9.3	10.6	-14.0
C-24-4	21.5	1.6	0.3	0.1	n.d.	n.d.	n.d.	n.d.	11.6	13.8	n.d.
C-24-5	24.5	1.5	0.4	0.1	n.d.	n.d.	10.6	7.5	13.1	15.2	-14.1
C-24-6	38.0	0.9	0.7	0.1	n.d.	n.d.	8.8	7.6	17.0	22.6	-14.7
C-24-7	62.0	0.5	0.3	0.1	n.d.	n.d.	n.d.	n.d.	21.2	28.9	n.d.
C-24-8	89.0	0.3	0.1	n.d.	n.d.	n.d.	5.3	8.8	24.5	30.0	-15.5
C-24-9	94.0	0.2	0.1	n.d.	n.d.	n.d.	n.d.	n.d.	36.4	41.0	n.d.
C-24-10	96.0	0.0	0.0	n.d.	n.d.	n.d.	7.8	n.d.	n.d.	n.d.	n.d.
C-24-blank	188.0	0.0	0.0	n.d.	n.d.	n.d.	14.3	n.d.	n.d.	n.d.	n.d.
H-24-1	13.8	2.1	0.1	0.1	n.d.	n.d.	14.7	n.d.	10.3	9.5	-18.3
H-24-2	15.0	1.8	0.3	0.1	n.d.	n.d.	13.4	9.1	15.2	12.7	-18.3
H-24-3	15.5	1.7	0.6	n.d.	n.d.	n.d.	n.d.	n.d.	12.3	5.8	n.d.
H-24-4	15.8	1.9	0.5	n.d.	n.d.	n.d.	n.d.	n.d.	12.4	6.3	n.d.
H-24-5	17.8	1.2	0.8	0.0	n.d.	n.d.	11.8	n.d.	34.5	25.1	-17.7
H-24-6	18.0	1.5	1.0	n.d.	n.d.	n.d.	n.d.	n.d.	23.3	15.9	n.d.
H-24-7	20.0	0.8	1.5	n.d.	n.d.	n.d.	n.d.	n.d.	37.0	20.7	n.d.
H-24-8	22.5	0.0	1.2	0.0	n.d.	n.d.	12.5	8.6	n.d.	n.d.	-19.2
H-24-9	38.5	0.0	0.0	0.2	n.d.	n.d.	14.7	9.9	n.d.	n.d.	-20.0
H-24-blank-1	4.0	0.1	0.0	0.0	n.d.	n.d.	n.d.	n.d.	n.d.	n.d.	n.d.
H-24-blank-2	38.5	0.0	0.0	n.d.	n.d.	n.d.	16.9	1.8	n.d.	n.d.	n.d.
S-24-1	13.0	2.2	0.0	0.2	n.d.	n.d.	14.7	9.9	7.8	8.0	-13.0
S-24-2	13.3	2.1	0.1	n.d.	n.d.	n.d.	n.d.	n.d.	n.d.	n.d.	-11.4
S-24-3	14.0	1.8	0.3	n.d.	n.d.	n.d.	15.7	7.3	11.9	10.3	-11.6
S-24-4	14.8	1.7	0.3	n.d.	n.d.	n.d.	n.d.	n.d.	n.d.	n.d.	n.d.
S-24-5	15.5	1.8	0.3	0.3	n.d.	n.d.	18.2	7.4	17.2	17.5	-12.0
S-24-6	17.5	0.3	1.3	n.d.	n.d.	n.d.	13.2	n.d.	59.4	60.8	n.d.
S-24-7	18.5	0.3	1.3	0.1	n.d.	n.d.	n.d.	n.d.	61.1	73.8	n.d.
S-24-8	19.5	0.2	1.4	n.d.	n.d.	n.d.	n.d.	n.d.	62.0	76.1	n.d.
S-24-9	21.0	0.0	1.4	0.1	n.d.	n.d.	n.d.	n.d.	n.d.	n.d.	n.d.
S-24-10	22.3	0.0	1.5	n.d.	n.d.	n.d.	15.9	8.0	n.d.	n.d.	-11.2
S-24-11	23.8	0.0	1.1	n.d.	n.d.	n.d.	n.d.	n.d.	n.d.	n.d.	n.d.
S-24-12	38.5	0.0	0.0	1.0	n.d.	n.d.	18.5	8.7	n.d.	n.d.	-10.5
S-24-blank-1	38.5	0.1	0.0	0.0	n.d.	n.d.	27.3	n.d.	n.d.	n.d.	n.d.
CW water	0.0	1.9	0.0	n.d.	n.d.	n.d.	n.d.	n.d.	5.9	8.0	n.d.
S-16-1	25.0	1.8	0.2	n.d.	0.8	0.001	n.d.	n.d.	17.4	14.3	n.d.
S-16-2	27.0	1.3	0.1	n.d.	0.6	0.001	n.d.	n.d.	20.5	20.5	n.d.

S-16-3	30.0	1.0	0.5	n.d.	n.d.	n.d.	n.d.	n.d.	28.7	29.8	n.d.
S-16-4	32.0	0.6	0.8	n.d.	2.5	0.002	n.d.	n.d.	46.2	39.7	n.d.
S-16-5	34.0	0.3	1.2	n.d.	n.d.	n.d.	n.d.	n.d.	62.1	68.6	n.d.
S-16-6	39.0	0.0	1.7	n.d.	8.7	0.009	n.d.	n.d.	n.d.	n.d.	n.d.
S-16-7	42.0	0.0	1.8	n.d.	1.9	0.002	n.d.	n.d.	n.d.	n.d.	n.d.
S-16-8	46.0	0.0	0.7	n.d.	0.4	0.000	n.d.	n.d.	n.d.	n.d.	n.d.
S-16-9	50.0	0.0	0.8	n.d.	1.1	0.001	n.d.	n.d.	n.d.	n.d.	n.d.
S-16-10	64.0	0.0	0.0	n.d.	n.d.	n.d.	n.d.	n.d.	n.d.	n.d.	n.d.
S-8'-1	66.0	1.6	0.0	n.d.	n.d.	n.d.	n.d.	n.d.	9.0	10.1	n.d.
S-8'-2	99.0	1.3	0.3	n.d.	n.d.	n.d.	n.d.	n.d.	13.6	13.0	n.d.
S-8'-3	114.0	0.9	0.3	n.d.	n.d.	n.d.	n.d.	n.d.	16.4	15.7	n.d.
S-8-1	66.0	1.7	0.1	n.d.	1.5	0.001	n.d.	n.d.	15.0	17.4	n.d.
S-8-2	75.0	1.2	0.2	n.d.	1.8	0.002	n.d.	n.d.	22.9	n.d.	n.d.
S-8-3	90.0	0.7	0.6	n.d.	2.0	0.002	n.d.	n.d.	24.3	20.6	n.d.
S-8-4	99.0	0.0	1.2	n.d.	5.1	0.005	n.d.	n.d.	n.d.	n.d.	n.d.
S-8-5	114.0	0.0	0.9	n.d.	2.8	0.003	n.d.	n.d.	n.d.	n.d.	n.d.
S-8-6	123.0	0.0	0.7	n.d.	0.0	0.000	n.d.	n.d.	n.d.	n.d.	n.d.
S-8-7	138.0	0.0	0.7	n.d.	3.4	0.003	n.d.	n.d.	n.d.	n.d.	n.d.
S-8-8	147.0	0.0	0.0	n.d.	0.6	0.001	n.d.	n.d.	n.d.	n.d.	n.d.
CW water	0.0	1.4	0.0	n.d.	n.d.	n.d.	0.5	n.d.	14.5	13.4	n.d.
DS-24-1	3.5	1.4	0.0	n.d.	n.d.	n.d.	n.d.	n.d.	n.d.	n.d.	n.d.
DS-24-2	5.5	1.3	0.1	0.1	n.d.	n.d.	2.2	n.d.	13.5	12.8	n.d.
DS-24-3	6.0	0.6	0.1	0.0	2.9	0.003	1.7	n.d.	25.2	23.9	n.d.
DS-24-4	7.5	0.8	0.3	n.d.	n.d.	n.d.	n.d.	n.d.	21.5	19.3	n.d.
DS-24-5	9.0	0.2	0.5	n.d.	1.6	0.002	1.9	n.d.	53.1	55.0	n.d.
DS-24-6	9.5	0.0	0.7	1.3	n.d.	n.d.	2.5	n.d.	n.d.	n.d.	n.d.
DS-24-7	10.5	0.6	0.4	n.d.	n.d.	n.d.	n.d.	n.d.	n.d.	n.d.	n.d.
DS-24-8	11.0	0.9	0.8	n.d.	5.4	0.005	n.d.	n.d.	26.7	28.6	n.d.
DS-24-9	12.5	0.0	0.3	n.d.	n.d.	n.d.	n.d.	n.d.	n.d.	n.d.	n.d.
DS-24-10	13.3	0.6	0.5	1.0	n.d.	n.d.	n.d.	n.d.	28.1	27.6	n.d.
DS-24-11	14.0	0.0	0.5	n.d.	n.d.	n.d.	1.7	n.d.	n.d.	n.d.	n.d.
DS-24-12	15.0	0.0	0.5	n.d.	n.d.	n.d.	n.d.	n.d.	n.d.	n.d.	n.d.
DS-24-13	17.0	0.6	0.5	n.d.	15.1	0.015	n.d.	n.d.	33.3	24.2	n.d.
DS-24-14	17.0	0.4	0.6	0.9	11.7	0.012	n.d.	n.d.	44.3	43.6	n.d.
DS-24-15	20.0	0.0	0.4	0.3	n.d.	n.d.	n.d.	n.d.	n.d.	n.d.	n.d.
DS-24-16	20.3	0.1	0.5	n.d.	12.7	0.013	n.d.	n.d.	78.5	70.7	n.d.
DS-24-17	22.0	0.0	0.6	n.d.	n.d.	n.d.	n.d.	n.d.	n.d.	n.d.	n.d.
DS-24-18	23.0	0.0	0.0	0.5	n.d.	n.d.	8.8	n.d.	n.d.	n.d.	n.d.
DS-24-19	24.0	0.0	0.2	n.d.	n.d.	n.d.	1.7	n.d.	n.d.	n.d.	n.d.

* % of initial NO₃⁻-N found as N₂O-N

n.d. = non determined

NH₄⁺ in the DS-24 experiment was analyzed by ion selective electrode while in the others by spectrophotometry

Table S4. ICP data. Major cations and trace elements concentration measured in the samples from the laboratory experiments (semiquantitative).

Code	Hour	Na	S	Ca	Mg	K	Si	Sr	P	B	Li	Mn	Zn	Cu	Fe	Ba	V	Co	Tl	Cd	Cr
CW water	0.0	326.8	146.3	130.7	99.3	6.2	10.9	4.2	-	0.35	0.12	-	-	0.08	0.01	0.06	0.06	0.01	0.14	-	0.01
C-24-1	14.0	345.0	163.0	125.8	103.4	65.4	11.4	3.9	1.4	0.42	0.13	0.05	0.09	0.04	0.10	0.05	0.07	-	-	-	-
C-24-2	14.5	334.6	151.1	125.4	101.2	43.3	11.1	3.9	0.8	0.39	0.13	0.05	0.06	0.04	0.07	0.05	0.07	0.01	-	-	-
C-24-3	20.0	321.8	151.8	124.0	100.4	58.2	10.9	3.8	1.0	0.40	0.12	0.06	0.07	0.03	0.08	0.05	0.07	-	0.15	-	-
C-24-5	24.5	328.7	160.1	123.2	102.8	68.7	11.3	3.8	1.2	0.42	0.13	0.08	0.11	0.04	0.11	0.05	0.07	-	-	-	-
C-24-6	38.0	325.2	152.3	123.1	104.6	51.6	11.4	3.6	1.4	0.41	0.13	0.11	0.11	0.04	0.12	0.04	0.07	-	-	-	-
C-24-8	89.0	334.2	151.7	125.6	104.5	41.5	12.1	3.6	1.4	0.40	0.13	0.12	0.05	0.05	0.07	0.04	0.07	-	-	0.01	-
H-24-1	13.8	360.3	168.3	139.4	102.3	160.1	22.8	4.3	0.6	0.38	0.13	0.04	0.04	0.03	0.02	0.11	0.07	0.02	-	0.01	-
H-24-2	15.0	362.0	165.3	139.5	105.0	130.8	22.2	4.2	2.3	0.38	0.13	0.05	0.04	0.03	0.02	0.24	0.06	-	-	-	-
H-24-5	17.8	371.4	170.9	141.4	103.0	142.1	22.1	4.3	-	0.38	0.13	0.06	0.05	0.03	0.01	0.11	0.06	-	-	-	-
H-24-8	22.5	365.1	169.0	140.9	103.4	180.9	25.1	4.3	-	0.37	0.13	0.06	0.06	0.03	0.02	0.16	0.07	0.01	-	-	-
H-24-9	38.5	355.7	164.3	140.4	104.1	167.2	31.2	4.4	0.8	0.37	0.13	0.04	0.06	0.03	0.01	0.13	0.06	-	-	-	-
S-24-1	13.0	318.9	155.5	136.2	108.1	130.8	13.4	4.0	1.2	0.48	0.12	0.10	0.09	0.07	0.06	0.08	0.07	-	-	-	-
S-24-2	13.3	324.5	146.8	128.6	101.5	75.5	13.6	3.8	1.6	0.36	0.12	0.11	0.05	0.05	0.04	0.07	0.06	0.01	-	-	-
S-24-3	14.0	325.3	148.8	126.4	101.4	118.2	13.0	3.7	2.2	0.38	0.12	0.13	0.03	0.04	0.04	0.07	0.06	-	0.15	-	-
S-24-5	15.5	329.9	151.8	130.2	103.2	78.9	14.4	3.8	1.4	0.39	0.12	0.17	0.03	0.04	0.04	0.08	0.06	-	-	-	-
S-24-10	22.3	318.4	149.4	130.9	104.5	108.7	13.9	3.8	0.8	0.39	0.13	0.12	0.04	0.05	0.04	0.12	0.07	-	-	-	-
S-24-12	38.5	329.2	150.0	139.0	109.9	99.5	14.4	4.0	1.1	0.39	0.13	0.16	0.04	0.06	0.05	0.10	0.07	0.03	-	-	0.01

All data is expressed as ppm. Hyphen = below detection limit. The Al, As, Be, Mo, Ni, Pb, Sb, Se and Ti were below detection limit in all analyzed samples.

Table S5. CW test results. Chemical and isotopic characterization of the samples collected in the CW previous and after the implementation of the bioremediation strategy.

Date	Point	NO ₂ ⁻ (mM)	NO ₃ ⁻ (mM)	NH ₄ ⁺ (mM)	DIC (mM)	NPDOC (mM)	SO ₄ ²⁻ (mM)	δ ¹³ C-DIC (‰)	δ ¹⁵ N- NO ₃ ⁻ (‰)	δ ¹⁸ O- NO ₃ ⁻ (‰)	δ ³⁴ S-SO ₄ ²⁻ (‰)	δ ¹⁸ O-SO ₄ ²⁻ (‰)	NO ₃ ⁻ attenuation			
													% ¹	% ²	kg/d	
14/06/17	H1	0.0	1.4	n.d.	7.1	n.d.	n.d.	n.d.	6.4	7.2	0.8	12.5	n.d.	n.d.	n.d.	
	H2	0.0	1.2	n.d.	6.9	n.d.	n.d.	n.d.	6.8	5.9	n.d.	n.d.	n.d.	n.d.	n.d.	
	H3	0.0	1.4	n.d.	6.8	n.d.	n.d.	n.d.	6.8	6.5	1.8	12.7	n.d.	n.d.	n.d.	
	H4	0.0	1.4	n.d.	n.d.	n.d.	n.d.	n.d.	n.d.	8.1	6.7	n.d.	n.d.	n.d.	n.d.	n.d.
	H5	0.0	1.4	n.d.	6.9	n.d.	n.d.	n.d.	n.d.	7.5	6.6	n.d.	n.d.	n.d.	n.d.	n.d.
	H6	0.0	1.2	n.d.	7.0	n.d.	n.d.	n.d.	n.d.	8.3	6.1	2.5	12.4	n.d.	n.d.	n.d.
05/09/17	H1	0.0	1.3	0.0	7.5	0.6	n.d.	-12.9	11.6	8.7	n.d.	n.d.	n.d.	n.d.	n.d.	
	H2	0.0	1.3	n.d.	7.3	0.5	n.d.	-12.7	n.d.	n.d.	n.d.	n.d.	n.d.	n.d.	n.d.	
	H3	0.0	1.5	0.0	7.4	0.4	n.d.	-12.7	19.2	18.2	n.d.	n.d.	n.d.	n.d.	n.d.	
	H4	0.0	1.5	n.d.	7.5	0.6	n.d.	-12.2	n.d.	n.d.	n.d.	n.d.	n.d.	n.d.	n.d.	
	H5	0.0	1.2	n.d.	7.3	0.5	n.d.	-12.8	n.d.	n.d.	n.d.	n.d.	n.d.	n.d.	n.d.	
	H6	0.0	1.1	0.0	7.3	0.5	n.d.	-12.4	9.6	7.1	n.d.	n.d.	n.d.	n.d.	n.d.	
12/09/17	H1	0.0	1.3	0.0	7.1	0.4	n.d.	-12.4	7.0	4.7	3.4	13.5	n.d.	n.d.	n.d.	
	H2	0.0	1.2	n.d.	7.5	0.5	n.d.	-12.8	n.d.	n.d.	n.d.	n.d.	n.d.	n.d.	n.d.	
	H3	0.0	0.9	0.0	7.1	0.5	n.d.	-12.5	14.9	11.8	3.6	13.8	n.d.	n.d.	n.d.	
	H4	0.0	0.8	n.d.	6.5	0.6	n.d.	-12.1	n.d.	n.d.	n.d.	n.d.	n.d.	n.d.	n.d.	
	H5	0.0	0.9	n.d.	6.4	0.6	n.d.	-11.8	n.d.	n.d.	n.d.	n.d.	n.d.	n.d.	n.d.	
	H6	0.0	1.0	0.0	6.6	0.5	n.d.	-12.0	17.1	13.0	3.1	13.1	n.d.	n.d.	n.d.	
02/10/17	H1	0.0	1.4	0.0	7.0	0.4	4.2	-12.7	9.7	8.4	n.d.	n.d.	0.0	0.0	n.d.	
	H2	0.1	1.1	n.d.	7.5	0.8	4.2	-11.8	13.7	12.4	n.d.	n.d.	26.5	16.8	n.d.	
	H3	0.1	0.4	0.0	8.2	1.3	3.7	-12.1	22.4	20.9	n.d.	n.d.	73.8	43.9	n.d.	
	H4	0.2	0.2	n.d.	8.9	1.9	4.5	-11.7	n.d.	n.d.	n.d.	n.d.	87.8	n.d.	n.d.	
	H5	0.2	0.2	n.d.	9.1	1.3	4.7	-12.0	n.d.	n.d.	n.d.	n.d.	87.8	n.d.	n.d.	

	H6	0.2	0.2	0.0	9.1	2.3	4.4	-13.1	32.9	29.9	n.d.	n.d.	86.3	64.0	78.4
10/10/17	H1	0.0	1.7	0.0	n.d.	0.4	3.7	-12.6	8.5	7.4	3.9	13.9	0.0	0.0	n.d.
	H2	0.0	1.3	n.d.	7.6	0.6	3.7	-12.0	11.7	11.0	n.d.	n.d.	23.8	14.2	n.d.
	H3	0.1	0.5	0.0	8.1	0.9	3.0	-11.4	15.1	14.4	4.3	12.9	72.9	26.6	n.d.
	H4	0.1	0.2	n.d.	8.7	1.6	3.0	-11.1	n.d.	n.d.	n.d.	n.d.	90.7	n.d.	n.d.
	H5	0.1	0.2	n.d.	8.8	1.1	3.9	-11.5	n.d.	n.d.	n.d.	n.d.	89.1	n.d.	n.d.
	H6	0.1	0.2	0.0	n.d.	1.1	3.9	-11.5	34.1	31.9	4.4	12.6	89.5	68.1	100.3
11/05/18	H1	0.0	1.1	0.0	6.9	0.7	3.9	n.d.	11.1	8.0	4.2	12.4	n.d.	n.d.	n.d.
	H2	0.0	1.2	n.d.	7.0	0.7	4.3	n.d.	n.d.	n.d.	n.d.	n.d.	n.d.	n.d.	n.d.
	H3	0.0	1.1	0.0	6.8	0.5	4.2	n.d.	n.d.	n.d.	4.3	12.1	n.d.	n.d.	n.d.
	H4	0.0	1.6	n.d.	0.0	0.5	5.2	n.d.	13.7	11.1	n.d.	n.d.	n.d.	n.d.	n.d.
	H5	0.0	1.3	n.d.	6.9	0.5	5.4	n.d.	13.5	10.7	4.4	12.1	n.d.	n.d.	n.d.
	H6	0.0	1.5	0.0	6.9	0.5	5.4	n.d.	12.7	11.2	n.d.	n.d.	n.d.	n.d.	n.d.
18/05/18	H1	0.0	1.6	0.0	7.1	0.5	5.7	n.d.	12.9	11.9	3.9	12.2	0.0	0.0	n.d.
	H2	0.0	1.5	0.0	7.2	0.6	5.6	n.d.	13.9	10.7	n.d.	n.d.	9.9	0.0	n.d.
	H3	0.1	0.8	0.1	0.0	0.7	5.7	n.d.	20.1	19.0	3.7	12.1	48.0	27.8	n.d.
	H4	0.1	0.2	0.3	8.0	1.3	5.5	n.d.	n.d.	n.d.	n.d.	n.d.	88.8	n.d.	n.d.
	H5	0.1	0.2	0.3	7.9	1.7	5.7	n.d.	32.4	28.2	n.d.	n.d.	88.8	55.8	n.d.
	H6	0.1	0.2	0.1	7.9	1.1	5.5	n.d.	33.9	32.1	3.9	12.2	85.7	61.0	84.5
25/05/18	H1	0.0	1.5	0.0	7.2	0.7	5.8	n.d.	14.0	13.8	3.6	12.4	0.0	0.0	n.d.
	H2	0.0	1.2	0.1	7.5	0.7	5.7	n.d.	11.9	9.5	n.d.	n.d.	21.3	0.0	n.d.
	H3	0.1	0.3	0.0	8.1	1.2	5.3	n.d.	22.4	19.7	4.2	11.8	79.9	27.7	28.1
	H4	0.0	0.0	0.1	9.4	1.6	4.4	n.d.	n.d.	n.d.	n.d.	n.d.	100.0	n.d.	n.d.
	H5	0.1	0.0	0.1	8.1	1.2	5.4	n.d.	n.d.	n.d.	3.9	11.8	100.0	n.d.	n.d.
	H6	0.1	0.0	0.0	8.3	1.0	5.2	n.d.	n.d.	n.d.	n.d.	n.d.	100.0	n.d.	n.d.
12/06/18	H1	0.0	1.2	0.0	0.0	0.8	4.2	n.d.	9.2	7.0	3.9	12.6	0.0	0.0	n.d.
	H2	0.0	1.2	0.0	7.4	0.6	4.3	n.d.	n.d.	n.d.	n.d.	n.d.	5.9	n.d.	n.d.
	H3	0.0	0.9	n.d.	7.3	0.6	4.2	n.d.	10.0	7.1	3.8	12.5	29.4	2.1	n.d.
	H4	0.0	0.8	0.0	0.0	0.6	4.2	n.d.	n.d.	n.d.	n.d.	n.d.	32.1	n.d.	n.d.

	H5	0.1	0.8	n.d.	0.0	0.8	4.3	n.d.	n.d.	n.d.	n.d.	n.d.	37.7	n.d.	n.d.
	H6	0.1	0.6	0.0	7.6	0.7	4.3	n.d.	16.3	12.9	3.9	12.4	51.2	25.8	27.1
13/07/18	H1	0.0	1.6	0.0	6.9	0.6	3.5	n.d.	8.4	6.1	n.d.	n.d.	0.0	0.0	n.d.
	H2	0.0	1.5	0.0	6.7	0.7	3.6	n.d.	n.d.	n.d.	n.d.	n.d.	9.7	n.d.	n.d.
	H3	0.0	1.6	0.0	7.1	0.6	3.4	n.d.	9.2	6.6	n.d.	n.d.	2.2	n.d.	n.d.
	H4	0.0	1.4	0.0	0.0	0.6	3.3	n.d.	n.d.	n.d.	n.d.	n.d.	12.0	n.d.	n.d.
	H5	0.1	1.2	n.d.	7.6	0.6	3.3	n.d.	n.d.	n.d.	n.d.	n.d.	27.8	n.d.	n.d.
	H6	0.1	1.0	0.0	0.0	0.6	3.3	n.d.	15.7	12.6	n.d.	n.d.	36.8	26.9	37.4
19/08/18	H1	0.0	1.1	n.d.	0.0	0.8	2.2	n.d.	7.7	5.4	4.7	12.2	0.0	0.0	n.d.
	H3	0.0	1.1	n.d.	0.0	0.6	2.2	n.d.	n.d.	n.d.	4.6	11.9	1.8	n.d.	n.d.
	H4	0.0	1.0	n.d.	7.8	n.d.	2.2	n.d.	n.d.	n.d.	n.d.	n.d.	7.0	n.d.	n.d.
	H5	0.0	1.0	n.d.	n.d.	n.d.	2.1	n.d.	n.d.	n.d.	n.d.	n.d.	4.5	n.d.	n.d.
	H6	0.0	1.0	n.d.	n.d.	0.7	2.1	n.d.	8.8	5.8	4.0	11.8	4.1	3.3	3.1
13/09/18	H1	0.0	1.6	n.d.	n.d.	0.5	2.4	n.d.	7.8	6.7	n.d.	n.d.	0.0	0.0	n.d.
	H2	0.0	1.5	n.d.	n.d.	n.d.	2.5	n.d.	n.d.	n.d.	n.d.	n.d.	5.7	n.d.	n.d.
	H3	0.0	1.3	n.d.	n.d.	0.6	2.5	n.d.	7.6	7.0	n.d.	n.d.	19.0	0.3	n.d.
	H4	0.0	1.3	n.d.	n.d.	n.d.	2.5	n.d.	7.9	10.6	n.d.	n.d.	19.7	8.5	n.d.
	H5	0.0	1.2	n.d.	n.d.	n.d.	2.5	n.d.	n.d.	n.d.	n.d.	n.d.	22.3	n.d.	n.d.
	H6	0.0	1.2	n.d.	n.d.	0.7	2.5	n.d.	9.2	7.6	n.d.	n.d.	24.7	5.0	6.9
19/10/18	H1	0.0	1.6	n.d.	n.d.	0.4	2.6	n.d.	6.7	4.5	n.d.	n.d.	0.0	0.0	n.d.
	H2	0.0	1.7	n.d.	n.d.	n.d.	2.5	n.d.	n.d.	n.d.	n.d.	n.d.	-1.4	n.d.	n.d.
	H3	0.0	0.5	n.d.	n.d.	0.7	2.6	n.d.	7.8	7.1	n.d.	n.d.	68.6	8.3	n.d.
	H4	0.0	1.5	n.d.	n.d.	n.d.	2.6	n.d.	n.d.	n.d.	n.d.	n.d.	8.7	n.d.	n.d.
	H5	0.0	1.5	n.d.	n.d.	n.d.	2.6	n.d.	n.d.	n.d.	n.d.	n.d.	6.6	n.d.	n.d.
	H6	0.0	1.4	n.d.	n.d.	0.4	2.6	n.d.	11.4	10.1	n.d.	n.d.	12.6	21.0	29.4

X¹ is calculated from concentration data while X² is calculated from isotopic data

n.d. = non determined

NH₄⁺ in the 2017 campaigns was analyzed by ion chromatography while in the 2018 campaigns by ion selective electrode